

Difficulty in chirality recognition for Transformer architectures learning chemical structures from string representations

Yasuhiro Yoshikai^{1,3} Tadahaya Mizuno^{1,2,3,4}
Shumpei Nemoto¹ Hiroyuki Kusuhara¹

¹ Laboratory of Molecular Pharmacokinetics, Graduate School of Pharmaceutical Sciences, The University of Tokyo, 7-3-1 Hongo, Bunkyo, Tokyo, Japan

² Author to whom correspondence should be addressed.

³ These authors contributed equally.

⁴ e-mail: tadahaya@gmail.com

Abstract

Recent years have seen rapid development of descriptor generation based on representation learning of extremely diverse molecules, especially those that apply natural language processing (NLP) models to SMILES, a literal representation of molecular structure. However, little research has been done on how these models understand chemical structure. To address this black box, we investigated the relationship between the learning progress of SMILES and chemical structure using a representative NLP model, the Transformer. We show that while the Transformer learns partial structures of molecules quickly, it requires extended training to understand overall structures. Consistently, the accuracy of molecular property predictions using descriptors generated from models at different learning steps was similar from the beginning to the end of training. Furthermore, we found that the Transformer requires particularly long training to learn chirality and sometimes stagnates with low performance due to misunderstanding of enantiomers. These findings are expected to deepen the understanding of NLP models in chemistry.

Introduction

Recent advancements in machine learning have influenced various studies in chemistry such as molecular property prediction, energy calculation, and structure generation¹⁻⁶. To utilize machine learning methods in chemistry, we first need to make computers recognize chemical structures. One of the most popular approaches is to use chemical language models, which are natural language processing (NLP) models fed with strings representing chemical structures such as simplified molecular input line entry specification

(SMILES)⁷. In 2016, Gómez-Bombarelli et al. applied a chemical language model using a neural network for descriptor generation and created a trend⁸⁻¹⁰. In this approach, a neural NLP model such as a recurrent neural network (RNN) learns an extremely wide variety of SMILES from public databases¹¹⁻¹³, converts the string into a low-dimensional vector, decodes it back to the original SMILES, and then the intermediate vector is drawn out as a descriptor. The obtained descriptor is superior to the conventional fingerprints, such as MACCS keys¹⁴ and ECFP¹⁵, in continuous and thus highly expressive natures, and that the original structures can be restored from the descriptor by the decoder¹⁶. On the other hand, the presented approach also has the disadvantage that it obscures the process of descriptor generation and that the meanings of each value in the descriptor are hard to interpret. It is scarcely studied how chemical language models understand structures of extremely diverse molecules and connect chemical structures and descriptors. Related works are described in Supplementary Note 1.

In this study, we tackle with addressing this black box by comparing the performance of the model and its descriptor at various steps of training, which clarifies what types of molecular features are easily incorporated into the descriptor and what types are not. Particularly, we focus on the most prevalent NLP model, the Transformer, a well utilized architecture for descriptor generation and other chemical language tasks these days¹⁷⁻³². To be specific, we train a Transformer model to translate SMILES strings and then compare perfect agreement and similarity of molecular fingerprints between prediction and target at different training steps. We also conduct 6 molecular property prediction tasks with descriptors generated by models at different steps in training and studied what kinds of tasks are easily solved. We further find that the translation accuracy of the Transformer sometimes stagnates at a low level for a while and then suddenly surges. To clarify the cause of this, we compare translation accuracy for each character of SMILES. Finally, we search for and found methods to prevent stagnation and stabilize learning.

Results

Partial/overall structure recognition of the Transformer in learning progress

To understand how the Transformer model learns the diverse chemical structures, we first researched the relationship between the learning procedure and the model performance by comparing the models at various training steps. In this study, we trained the Transformer to predict canonical SMILES of

molecules based on their randomized SMILES³²⁻³⁴. For models at various steps of training, we calculated *perfect accuracy* and *partial accuracy* of predicted SMILES expression³⁵. We supposed *perfect accuracy*, which evaluates the complete consistency of target and prediction, represents how much the models understand the connectivity of atoms constituting overall molecular structures, whereas *partial accuracy*, which measures position-wise accuracy of prediction, indicates recognition of the connectivity of atoms in partial structures. The result showed that *partial accuracy* rapidly converged to 1.0, meaning almost complete translation, whereas *perfect accuracy* gradually increased as the learning proceeded (Figure 1a). This result suggests that the Transformer model recognizes partial structures of molecules at quite an early stage of training when overall structures are yet to be understood well. To further evaluate partial and overall recognition of molecules, we prepared the models when *perfect accuracy* surpassed 0.2, 0.5, 0.7, 0.9, 0.95, and 0.98 and at steps 0, 4,000, and 80,000 (end of training). For models at these steps, we computed MACCS keys¹⁴ and ECFP¹⁵ (radius $R = 1, 2, 3$) of predicted/target molecules; and calculated the Tanimoto similarity for each prepared model. As these descriptors are widely accepted to represent typical partial structures of molecules, their similarity between target and prediction will help the comprehension of the model on partial structures of molecules. As a result, the Tanimoto similarity of molecular fingerprints saturated at nearly 1.0, meaning complete correspondence of fingerprint between prediction and target, when *perfect accuracy* was merely about 0.3 (Figure 1a, 1b). We also compared the Tanimoto similarity with the loss function (Figure 1b), and it was shown that the fingerprints corresponded almost completely when the loss had yet to be converged. Figure 1c shows valid examples of predicted molecules with their targets at early phase of training (step 4000). These results also support the early recognition of partial structures and late recognition of the overall structure of molecules by the Transformer model. We previously found that the GRU model, derived from NLP, has a similar tendency as this finding³⁵. It is then suggested that NLP models, when trained to chemical structures by learning SMILES, recognize partial structures of molecules at the early stage of training, regardless of their architecture. These findings can be explained as follows: When translating randomized SMILES into canonical SMILES, the model needs to reproduce the numbers of atoms in the molecule with each atomic type and how they are bound together. Assuming that the numbers of atoms are easily learned as simple frequency distributions, a large part of the training is spent learning and reproducing the bonds between atoms. The model in the early phase of training can only reproduce easy-to-understand bonds between

atoms (such as those with high frequency and few other options), and those partially connected atoms are observed as partial structure. The model in the subsequent phase of training learns the remaining bonds which are left to be challenging tasks for the model but necessary for reconstructing the overall structures.

We also investigated what type of substructure is easily or hardly understood by the model using dimension-wise similarities of MACCS keys, whose details are written in Supplementary Note 2. No remarkable tendency was observed in the results, and the similarities of most of the dimensions converged rapidly.

Downstream task performance in the learning progress

Molecular descriptors are frequently used in solving cheminformatics tasks. Therefore, in many cases, the performance of descriptor generation methods is evaluated by how much downstream tasks, such as prediction of molecular properties, are solved from their descriptor. On the other hand, we have shown in a previous study that in the case of a descriptor generated by chemical language model based on GRU, downstream task performance is mainly related to the recognition of partial structures of molecules³⁵, and here we worked on the evaluation of the downstream task performance over the learning progress about the Transformer model. To be specific, we predicted the molecular properties from intermediate representation of molecules during translation in the Transformer at different steps. The details of descriptor generation and conditions of prediction are described in Molecular property prediction Section. Note that to evaluate the performance of memory expression itself, rather than the inherent architecture of the model, we did not conduct fine-tuning. We used benchmark datasets from MoleculeNet³⁶ summarized in Table 1.

Figure 2 and Supplementary Figures 1 and 2 show the prediction scores of each descriptor (also summarized in Table 2). The results showed that descriptors of models at an early phase, or even at the beginning of training, can perform just as well as that of the fully trained model, except for the prediction of Lipophilicity, although the score for this task saturated at an early phase (step 6,000). Duvenaud et al.³⁷ showed that neural fingerprint (NFP), a deep-learning and graph-based descriptor, correlated to ECFP and was able to predict molecular properties without training. Similarly, one of the explanations of the presented result is that the Transformer model, even with its initial weights, generates a meaningful descriptor by its inherent mechanism such as self-attention. This implies that the modifying structure of

the model is more helpful for improving the performance than changing what data the model is fine-tuned on. Note that the performance of the descriptor pooled from the Transformer memory is almost similar to that of ECFP and is slightly lower than that of CDDD. One of explanations of slightly low performance can be that the pooling process in descriptor generation omitted part of the structural information of molecules which is scattered in the whole memory. The potential for further structural enhancements in prediction, like co-learning of molecular properties, is worth noting although it falls outside the scope of this current study.

Stagnation of perfect accuracy in learning chemical structures

We experimented with different random seeds to reproduce the results in Partial/overall structure recognition of the Transformer in learning progress. It was then observed that the perfect accuracy of the Transformer sometimes stagnated at a low level for a while and then abruptly increased at a certain step. We are interested in this phenomenon and conducted some experiments changing the randomly determined conditions. To be specific, we trained the model with 14 different initial weights and 2 different orders of iteration on the training dataset. Figure 3a shows the perfect accuracy in these different conditions. The figure shows that while perfect accuracy uneventfully converges in many cases perfect accuracy sometimes stayed at ~0.6 from approximately 10,000 to 70,000 steps and then surged to nearly 1.0 or even maintained a low accuracy until the end of training. Figure 3b shows change of loss in conditions in which stagnation did or did not occur. This shows that the loss sharply decreased at the same time as accuracy surged.

To specify the determinative factor of the stagnation, we obtained the steps when accuracy exceeded 0.7 and 0.95, named *step-0.7* and *step-0.95* respectively. Based on Figure 3a, we considered *step-0.7* to represent the step when stagnation was resolved, and *step-0.95* is the step when learning was almost completed. Supplementary Figure 3a and 3b shows the relationship between *step-0.7/0.95* of the same seed and different iteration orders. The result shows that the trend of learning progress is similar for different iteration orders when the same initial weight was used. Supplementary Figure 3c and 3d shows the average *step-0.7/0.95* of each iteration order, and no significant difference of *step-0.7/0.95* was observed. These results suggest that whether the stagnation occurs or not depends on initial weight, rather than iteration order.

We replicated the experiments in Sections Partial/overall structure recognition of the Transformer in learning progress and Downstream task performance in the learning progress for one training in which stagnation occurred. We investigated the agreement of fingerprints and performance on downstream tasks at different steps of the learning with stagnation. As a result, the tendencies in found in the previous sections was conserved even when stagnation occurred, reinforcing our findings in the previous sections. Details about these experiments are shown in Supplementary Note 3.

Cause of stagnation in learning chemical structures

What is the cause of this stagnation? We investigated the model performance on each character of SMILES strings using 2 metrics. The first one is the perfect accuracy when each character is masked. This is calculated like perfect accuracy defined in Partial/overall structure recognition of the Transformer in learning progress Section except that prediction for a certain type of characters in the target is not considered. This value is expected to rise when a difficult, or commonly mistaken character is masked. The second metric is the accuracy of each character of the target when teacher forcing is used. In the test phase, as the model usually predicts each letter of SMILES from a previously predicted string, the model is likely to make an additional mistake when it has already made one. This means characters that appear more in the later positions (like “)”) compared with “(”) tend to show low accuracy. To remedy this, we adopted teacher-forcing³⁸ to predict the SMILES, meaning the model always predicts each letter from the correct SMILES string, when computing the accuracy of each character.

Figure 4a shows the transition of masked accuracy about training with or without stagnation. The results show that when the model is in stagnation, predictions of “@” and “@@” are wrong by a large number. These 2 characters are used to describe chirality in SMILES representation (Figure 4b). It suggests that stagnation was caused by confusion in discriminating enantiomers, and the subsequent surge of perfect accuracy was the result of the resolution of this confusion. We also investigated the ratio of correct predictions, wrong predictions due solely to chirality, and wrong predictions due to other reasons. Figure 4c shows that most of the mistakes in stagnation are due to chirality, which supports the impact of chirality confusion in stagnation.

It should be noted that errors occurred in both directions, involving mistakes of the “@” token for “@@”, and vice versa (Supplementary Figure 4a). Additionally, we conducted an analysis of the

accumulated count of "@" and "@@" tokens in the training set. As depicted in Supplementary Figure 4b, the occurrence of the "@@" token surpasses that of the "@" token in the target SMILES (canonical SMILES), while the difference appears to be marginal. In light of this observation, it is worth noting that stagnation did occur in some cases even when we took measures to train the model on a dataset that was well-balanced in terms of "@" and "@@" tokens (Supplementary Note 4). These findings underscore that bias regarding chiral token is not the primary cause of stagnation.

The true challenge for a chemical language model lies not in mastering the numerous elementary atom-bonding rules, but rather in comprehending the difficult rules that persist even after the basics have been acquired, which is consistent with Ucak's work regarding the reconstruction of molecular representations from fingerprints³⁹. The above findings indicate that learning chirality, which is the cause of stagnation, is the very difficult task for the Transformer model learning diverse chemical structures. Notably, the examination of the accuracy transition for each character not only confirmed that "@" and "@@" show a slower increase of accuracy than the other characters, but also revealed the difficulty of chiral tokens even when learning proceeds smoothly without stagnation (Supplementary Figure 5). This trend holds true considering character frequencies (Supplementary Figures 6 and 7). In addition, the accuracy for chiral tokens is relatively low even when the model reaches a plateau, a perfect accuracy of 0.9. It should be noted that the accuracy increase of "\\" token, related to geometrical isomers, was also slow (Supplementary Figure 5). This suggests that the tokens associated with stereochemistry pose a general challenge for the Transformer model in terms of learning, while the influence of geometrical isomers remains relatively modest, owing to their infrequent occurrence (approximately 1/100th of the chiral tokens).

These findings indicate that chirality of molecules is difficult for the Transformer to understand, and sometimes the model is confused about it for a long period, causing stagnation.

Solution of stagnation in learning chemical structures

Then, how can we facilitate the understanding of the Transformer on chirality? To answer this question, we applied the following perturbation to the learning process and evaluated its effect on stagnation.

1. Increase chirality in training dataset: It is possible that learning more enantiomers encourages the model to understand chirality. We therefore omitted half of the molecules in the training set whose SMILES has neither "@" nor "@@" and trained the model with the data in which chirality appears more frequently.

2. Introduce AdamW: In deep-learning studies, one of the possible explanations for this kind of stagnation is that the model is stuck to a local optimum, and changing the optimizer can be a solution to avoid such stagnation. We have been using the Adam optimizer based on Vaswani et al.³¹ so far, but here we tried the AdamW⁴⁰ optimizer. The AdamW optimizer is a refined optimizer of Adam with L^2 normalization in the loss function. Loshchilov et al.⁴⁰ showed that this optimizer can be adopted to a wider range of learnings than Adam.

3. He normal initialization: Experiments in 4.3 suggested that stagnation occurs depending on the initial weight of models. Thus, changing the initialization of model weight would stabilize learning. Here we introduced He normal initialization, which is referred to as suitable for the ReLU activation function in the Transformer.

4. pre-LN structure: Pre-LN is a structural modification of the Transformer first proposed in Xiong et al.⁴¹ to stabilize learning. This method prevents vanishing gradients in the lower layer of the Transformer by ensuring that the residual connection is not affected by layer normalization, which can cause vanishing gradients. This method has been shown to stabilize the learning of the Transformer⁴¹.

All these perturbations were respectively introduced to the baseline model, and training was conducted 14 times with different initial weights for each modification, except for the introduction of He normal, which showed a significant delay in learning and was aborted when 5 studies were finished. Considering the computational cost, we stopped training when perfect accuracy reached 0.95.

Supplementary Figure 8a and 8b shows the average of *step-0.7/0.95*. In some cases where the accuracy did not reach 0.7/0.95, *step-0.7/0.95* was defined as 80,000 (end of training). The result showed that the introduction of pre-LN significantly accelerated the learning speed, whereas other modifications did not achieve improvement. Figure 5a shows the changes in accuracy over time in the 14 trainings with pre-LN, compared with those about the control model. This figure also demonstrates that pre-LN strongly stabilizes learning.

Then, does pre-LN facilitate understanding of chirality, or simply accelerate overall learning? Figure 5b

and Supplementary Figure 9 show the masked accuracy and accuracy for each character in one of the studies in which pre-LN was adopted. The results show that while learning on all tokens is accelerated, “@” and “@@” is relatively slow to be learned even in the model with pre-LN, suggesting that pre-LN accelerates the learning of not only chirality but also molecular structure in general.

Investigation with another chemical language

Finally, to clarify the generalizability of our findings about the Transformer, we trained the model with another expression of molecules. Instead of SMILES, here we used InChI, an alternative literal representation of molecules adopted in some cheminformatics studies with chemical language models. Although the performances of chemical language models fed with InChI are reported to be inferior to those with SMILES^{10,42}, and therefore InChI expression is not used frequently, the translation task between InChI and SMILES guarantees that the model learns to extract essential connectivity of atoms constituting molecules because these representations are completely different, whereas randomized SMILES and canonical SMILES follows the same grammar. The details about InChI-to-SMILES translation are written in Supplementary Note 5.

The result showed early saturation of partial accuracy and fingerprint similarity compared to perfect accuracy and loss function, indicating that the recognition of partial structures is easier than overall structures in InChI-to-SMILES translation (Figures 6a and 6b). The performance on downstream tasks was not improved by training (Supplementary Figures 10 and 11). The results also revealed that the stagnation did occur in InChI-to-SMILES translation (Figure 6a), and character-wise analysis exhibited that confusion in discriminating enantiomers caused it (Figure 6c, 6d and Supplementary Figure 12). In addition, pre-LN introduction relieved the stagnation (Figures 6e), and character-wise accuracy showed overall acceleration of saturation and relatively low accuracy of chiral tokens when pre-LN was adopted, indicating that this structure generally accelerates understanding of chemical structures (Supplementary Figure 13). These results suggest that what we have found about the Transformer model trained by random-to-canonical SMILES translation is an innate property of Transformer, rather than a grammatical or processive problem specific to SMILES.

Discussion

In recent years, a new field of research has been established in which NLP models, especially the Transformer model, is applied to literal representations of molecules like SMILES to solve various tasks handling molecular structures: chemical language models with neural network⁷. In this paper, as a basic study of chemical language models for descriptor generation, we investigated how a Transformer model understands diverse chemical structures during the learning progress. We compared the agreement between the output and the target, and the fingerprints related to substructures, for the models in the process of learning. The performance of the descriptor generated by the model under training was also examined on the downstream tasks of predicting molecular properties. We further found that perfect accuracy of translation sometimes stagnates at a low level depending on the initial weight of the model. To find the cause of this phenomenon, we compared the accuracy per each character of SMILES, and we experimented with 4 alterations to prevent stagnation. The major findings in this paper are as follows:

1. In the Transformer model, partial structures of molecules are recognized in the early steps of training, whereas recognition of the overall structures requires more training. Together with our previous study about RNN models³⁵, this finding can be generalized for various NLP models fed with SMILES strings. Therefore, enabling the Transformer model to refer to overall structural information as an auxiliary task in its structure would help improve the descriptor generation model.
2. For molecular property prediction, the performance of the descriptor generated by the Transformer model may already have been saturated before it was trained, and it was not improved by the subsequent training. This suggests that the descriptor of the initial model already contains enough information for downstream tasks, which is perhaps the partial structures of molecules. On the other hand, it is also possible that downstream tasks like property prediction of molecules are too easy for the Transformer and inappropriate for evaluating Transformer-based descriptor generation methods.³¹
3. Translation performance of the Transformer concerning chirality is relatively slow to rise compared to the other factors, such as overall structures or other partial structures, and the model is sometimes

confused about chirality for a long period, causing persistent stagnation in whole structure recognition. This suggests that additional structures or tasks that teach chirality to the model can improve the performance of the model and its descriptor.

4. Introducing the pre-LN structure accelerates and stabilizes learning, including chirality.

These discoveries contribute to clarify the black box in chemical language models and are expected to activate this field. It is an intriguing future task to investigate whether these findings hold true in chemical language models for other applications with supervised natures such as structure generation and end-to-end property prediction, although we focused on descriptor generation in this study because this task makes the model purely learn chemical structures in an unsupervised manner. Chemical language models would be increasingly developed, as NLP is one of the most advanced fields in deep learning. On the other hand, there are many unknowns in the relationship between language models and chemical structures compared to prevalent neural network models in the field of chemistry, such as graph neural networks^{43,44}. Further basic research on the relationship between NLP models and chemical structures is expected to further clarify the black box about how NLP models evolve and recognize chemical structures, leading to the development and performance improvement of chemical language models for various tasks in chemistry.

Methods

Training a Transformer

Dataset

To pretrain a Transformer model, molecules were sampled from the ZINC-15 dataset¹¹, which contains approximately 1 billion molecules. After rough sampling of molecules from the whole dataset, Molecules with atoms other than H, B, C, N, O, F, P, S, Cl, Br, or I, and molecules that have more than 50 or less than 3 heavy atoms were filtered out, 30,190,532 (approximately 30M) molecules were sampled for train and test set. The molecules were sampled not randomly, but in a stratified way in terms of SMILES length

to reduce the bias of molecular weights and SMILES lengths in the training set, i.e., all molecules in ZINC-15 were classified according to lengths of SMILES strings, and 460,000 molecules were sampled from each length. All molecules were sampled for lengths which do not contain more than 460,000 molecules. The initial rough sampling was also stratified similarly not to omit molecules with rare length of SMILES. About 3% (9,057) molecules were sampled as the test set, and the remaining molecules were used for training. Note that random sampling is widely used instead of this stratified sampling, although we believe that our sampling strategy enables fair training of molecular structures with regard to molecular weight and SMILES length. We therefore conducted the key experiments with the dataset prepared by random sampling to confirm generality and obtained similar results. The details about these experiments are written in Supplementary Note 6.

The remaining molecules were then stripped of small fragments, such as salts, and canonical SMILES and randomized SMILES of them were generated. SMILES is a one-dimensional representation of a molecule, and because any atom can be the starting point, multiple SMILES representations correspond to a single molecule. To identify one specific representation, there is a rule for selecting the initial atom, and the SMILES representation identified based on this rule is called canonical SMILES, whereas the others are referred to here as randomized SMILES. Translation between randomized and canonical SMILES is used as a training task in ^{32,34}. We generated randomized SMILES by renumbering all atoms in molecule^{32,33}. InChI, another string representation of molecules were also generated for translation. All of these processes were conducted using the RDKit library (ver. 2022.03.02).

Model architecture

We implemented the model with PyTorch framework (ver. 1.8, except for the model with pre-LN structure). Parameters and model architecture were determined according to the original Transformer in ³¹; the dimension of the model was 512, the dimension of the feed-forward layer was 2,048, and the number of layers in the encoder and decoder was 6. We used ReLU activation, and the dropout ratio was 0.1 in both the encoder and the decoder.

Learning procedure

Randomized SMILES strings of molecules in the training dataset were tokenized and then fed into the

encoder of the Transformer. Tokenization was conducted with the vocabulary shown in Supplementary Table 1. “<s>” and “<\s>” tokens are added to the beginning end and of the token sequences, respectively, and “<pad>” tokens are added to some of the sequences to arrange the length of them in a batch.

Positional encoding was added to the embedded SMILES tokens. The input of the decoder was canonical SMILES strings of the same molecule, and the model was forced to predict the same canonical SMILES shifted by one character before, with the attention from posterior tokens being masked. Hence, the model was forced to predict each token of SMILES based on its prior tokens (teacher-forcing³⁸). We calculated cross-entropy loss for each token except the padding token, and the mean loss along all tokens was used as the loss function. As for translation from InChI to canonical SMILES, the vocabulary in Supplementary Table 2 was used for tokenization.

25,000 tokens were inputted per step following³¹. Due to resource restriction, the batch size was set to 12,500 tokens, and the optimizer was stepped after every 2 batches. We introduced bucketing^{10,31}, that is, we classified SMILES strings in training data into several ranges of their lengths, and generated batches from SMILES in the same range of length to reduce padding. The number of batches in total amounted to 147,946 (for 73,973 steps). We used Adam optimizer⁴⁵ with a warmup scheduler (warmup step = 4,000) and continued training up to 80,000 steps (slightly longer than one epoch), although training was aborted when *perfect accuracy* (described below) reached 0.95 in some studies to save time in training.

Metrics

We measured the translation performance of each model by 2 metrics: *perfect accuracy* and *partial accuracy*³⁵. *Perfect accuracy* means the ratio of molecules whose target SMILES strings were completely translated by the model, except those after end-of-string tokens (i.e., padding tokens). *Partial accuracy* means the character-wise ratio of coincidence between the target and predicted strings.

To evaluate recognition of the model about partial structures of molecules, we calculated MACCS keys and ECFP for both target and predicted SMILES and calculated the Tanimoto similarity of these fingerprints between them for the test set. The radius of ECFP was varied from 1 to 3. Because prediction of the Transformer does not always output valid SMILES, molecules for which the Transformer predicted invalid SMILES at any step were omitted when calculating Tanimoto similarity. Note that a valid SMILES means a grammatically correct SMILES which encodes a molecule that satisfies the octet rule.

We calculated the agreement of MACCS keys between the predicted and target molecules in each dimension. For each dimension, the percentage of molecules was calculated for which the model makes valid predictions and for which the predicted molecules have MACCS keys of 1, in all molecules that have MACCS keys of 1. The same percentage for bit 0 was also calculated.

Molecular property prediction

Dataset

Physical and biological property data of molecules was obtained from MoleculeNet³⁶ with the DeepChem module⁴⁶. Table 1 shows the datasets we used and their information. The same filtering and preprocessing were applied as in Training a Transformer Section to molecules in each dataset, although too long or short SMILES were not removed in order not to overestimate the prediction performance, and then duplicated SMILES were omitted. The model was trained and evaluated for 5 train-validation-test folds split by method recommended by DeepChem.

Molecular property prediction task

We tested the property prediction ability for models at steps when perfect accuracy reached 0.2, 0.5, 0.7, 0.9, 0.95, and 0.98 and at steps 0, 4,000, and 80,000 (end of training). In the property prediction experiments, only the encoder of the Transformer was used. Randomized SMILES were inputted into it, and then the memory (= output of encoder) was pooled and used as the descriptor of molecules. To minimize the effect of the pooling procedure, we tested 4 pooling methods: 1) average all memory along the axis of SMILES length, 2) extract memory corresponding to the first token in SMILES, 3) obtain the average and maximum memory along the axis of the SMILES length and concatenate them with the memories of the first and last token³⁴, 4) concatenate average, maximum, minimum, standard deviation, beginning, and end of memory. Note that the dimensions of pooled descriptors are not equal: 1) 512, 2) 512, 3) 2,048, and 4) 3,072.

From these pooled descriptors, we predicted the target molecular properties with SVM, XGBoost, and MLP in our preliminary study and chose XGBoost which showed the best performance. For each of the 5 splits, we searched hyperparameters by Bayesian optimization using Optuna⁴⁷. As baseline descriptors, we calculated ECFP (R = 2, dimension = 2,048) and CDDD¹⁰ (dimension = 512) for molecules in

MoleculeNet datasets and measured the property prediction accuracy. Random values from a uniform distribution in [0, 1] were generated and also used as baseline descriptors (dimension = 2,048).

Furthermore, we compared the prediction performance with Uni-Mol⁴⁸, one of the state-of-the-art models in molecular property prediction. The experiments were conducted for 5 folds split by the methods recommended by DeepChem, and the accuracy of prediction was measured by the recommended metric by MoleculeNet.

Experiment in different initial weight and iteration order

14 different initial weights were randomly generated with different random seeds in PyTorch, and 2 different orders of data iteration were made by randomly sampling molecules for each batch and randomly shuffling the batch iteration order with 2 different seeds. All hyperparameters were fixed during these 28 experiments in total. To perform numerous experiments, we aborted the experiments when accuracy reached 0.95 instead of continuing until step 80,000, except 4 experiments to see saturation. We calculated perfect accuracy and partial accuracy on validation set for every 2000 steps, and the step when perfect accuracy first reached 0.7/0.95 was called *step-0.7/0.95*, respectively. The mean *step-0.7* and *step-0.95* were compared between 2 iteration orders by two-sided Welch's t-test.

Research for the cause of stagnation

For each character in the vocabulary, we calculated the perfect accuracy with characters of each kind masked. This means we did not check whether the characters of the selected kind were correctly predicted by the Transformer when calculating perfect accuracy. We computed partial accuracy for each character as well. Because the Transformer predicts each character from memory and previous characters it predicted, it is more likely to produce wrong predictions after it once made a mistake. We therefore adopted teacher-forcing when calculating this metric, meaning the model predicts each character with the correct preceding characters³⁸. We examined the percentage of SMILES that could not be translated completely, for which the mistake was solely attributable to chirality. Since chirality of molecules is represented by "@" and "@@" tokens in SMILES, the percentage of molecules that were answered correctly except that "@" was mistaken for "@@", "@@" was mistaken for "@", or both, among all molecules were calculated.

Structural modifications of the model to prevent stagnation

For AdamW, He normal initialization, and pre-LN (pre-layer normalization) structures, we used PyTorch implementation. As pre-LN is not implemented in PyTorch version 1.8, we conducted experiments with the pre-LN structure in version 1.10. For experiments with more “@” and “@@”, training data was sampled again from the training dataset we prepared in Training a Transformer Section. SMILES strings that have either “@” or “@@” were sampled at 100% probability, and those that do not were sampled at 50%. The new training dataset contained about 135,000 molecules (about 67,500 steps). We did not change the test set.

These modifications were introduced respectively, and the model was trained from 14 initial weights. The number of steps the model took until perfect accuracy reached 0.7 and 0.95 was compared to the control experiment with no modification by two-sided Welch’s t-test with Bonferroni correction. Since we had to conduct many experiments in this section, we aborted experiments when accuracy reached 0.95 instead of continuing until step 80,000.

Data Availability

ZINC-15¹¹ dataset used to train and evaluate the model was downloaded from <https://zinc15.docking.org/> MoleculeNet³⁶ dataset used to evaluate performance of molecular property prediction was downloaded through DeepChem⁴⁶ module (<https://deepchem.io/>). Source data are provided with this paper.

Code Availability

Used codes and trained models are available at: <https://github.com/mizunogroup/ChiralityMisunderstanding>⁴⁹

References

1. Chen, H., Engkvist, O., Wang, Y., Olivecrona, M. & Blaschke, T. The rise of deep learning in drug discovery. *Drug Discov Today* **23**, 1241–1250 (2018).
2. Wu, Y. & Wang, G. Machine learning based toxicity prediction: From chemical structural description to transcriptome analysis. *Int J Mol Sci* **19**, (2018).
3. Butler, K. T., Davies, D. W., Cartwright, H., Isayev, O. & Walsh, A. Machine learning for molecular and materials science. *Nature* **559**, 547–555 (2018).

4. Danishuddin, Kumar, V., Faheem, M. & Woo Lee, K. A decade of machine learning-based predictive models for human pharmacokinetics: Advances and challenges. *Drug Discov Today* **27**, 529–537 (2022).
5. Khamis, M. A., Gomaa, W. & Ahmed, W. F. Machine learning in computational docking. *Artif Intell Med* **63**, 135–152 (2015).
6. Faber, F. A. *et al.* Prediction Errors of Molecular Machine Learning Models Lower than Hybrid DFT Error. *J Chem Theory Comput* **13**, 5255–5264 (2017).
7. Ikebata, H., Hongo, K., Isomura, T., Maezono, R. & Yoshida, R. Bayesian molecular design with a chemical language model. *J Comput Aided Mol Des* **31**, 379–391 (2017).
8. Gómez-Bombarelli, R. *et al.* Automatic chemical design using a data-driven continuous representation of molecules. *ACS Cent Sci* **4**, 268–276 (2018).
9. Quan, Z. *et al.* A System for Learning Atoms Based on Long Short-Term Memory Recurrent Neural Networks. in *2018 IEEE International Conference on Bioinformatics and Biomedicine (BIBM)* 728–733 (2018).
10. Winter, R., Montanari, F., Noé, F. & Clevert, D.-A. Learning continuous and data-driven molecular descriptors by translating equivalent chemical representations. *Chem Sci* **10**, 1692–1701 (2019).
11. Sterling, T. & Irwin, J. J. ZINC 15–ligand discovery for everyone. *J Chem Inf Model* **55**, 2324–2337 (2015).
12. Kim, S. *et al.* PubChem substance and compound databases. *Nucleic Acids Res* **44**, D1202–D1213 (2016).
13. Mendez, D. *et al.* ChEMBL: towards direct deposition of bioassay data. *Nucleic Acids Res* **47**, D930–D940 (2019).
14. Durant, J. L., Leland, B. A., Henry, D. R. & Nourse, J. G. Reoptimization of MDL Keys for Use in Drug Discovery. *J Chem Inf Comput Sci* **42**, 1273–1280 (2002).
15. Rogers, D. & Hahn, M. Extended-Connectivity Fingerprints. *J Chem Inf Model* **50**, 742–754 (2010).
16. Le, T., Winter, R., Noé, F. & Clevert, D.-A. Neuraldecipher–reverse-engineering extended-connectivity fingerprints (ECFPs) to their molecular structures. *Chem Sci* **11**, 10378–10389 (2020).
17. Bagal, V., Aggarwal, R., Vinod, P. K. & Priyakumar, U. D. MolGPT: molecular generation using a transformer-decoder model. *J Chem Inf Model* **62**, 2064–2076 (2021).
18. Hong, Y.-B., Lee, K.-J., Heo, D. & Choi, H. Molecule Generation for Drug Discovery with New Transformer Architecture. Preprint at <https://ssrn.com/abstract=4195528> (2022).
19. Rahimovich, D. R., Qaxramon O’g’li, A. S., O’g, S. R. A. & others. Application of transformer model architecture in the new drugs design. in *2021 International Conference on Information Science and Communications Technologies (ICISCT)* 1–3 (2021).
20. Shin, B., Park, S., Bak, J. & Ho, J. C. Controlled molecule generator for optimizing multiple chemical properties. in *Proceedings of the Conference on Health, Inference, and Learning* 146–153 (2021).
21. Kim, H., Na, J. & Lee, W. B. Generative chemical transformer: neural machine learning of molecular geometric structures from chemical language via attention. *J Chem Inf Model* **61**, 5804–5814 (2021).
22. Yang, Q. *et al.* Molecular transformer unifies reaction prediction and retrosynthesis across pharma chemical space. *Chemical communications* **55**, 12152–12155 (2019).
23. Karpov, P., Godin, G. & Tetko, I. V. A transformer model for retrosynthesis. in *International Conference on Artificial Neural Networks* 817–830 (2019).
24. Zheng, S., Rao, J., Zhang, Z., Xu, J. & Yang, Y. Predicting retrosynthetic reactions using self-corrected transformer neural networks. *J Chem Inf Model* **60**, 47–55 (2019).
25. Tetko, I. v, Karpov, P., van Deursen, R. & Godin, G. State-of-the-art augmented NLP transformer models for direct and single-step retrosynthesis. *Nat Commun* **11**, 5575 (2020).
26. Mao, K. *et al.* Molecular graph enhanced transformer for retrosynthesis prediction. *Neurocomputing* **457**, 193–202 (2021).
27. Maziarka, Ł. *et al.* Molecule attention transformer. Preprint at

- <https://arxiv.org/abs/2002.08264> (2020).
28. Zhu, J. *et al.* Dual-view Molecule Pre-training. Preprint at <http://arxiv.org/abs/2106.10234> (2021).
 29. Shin, B., Park, S., Kang, K. & Ho, J. C. Self-Attention Based Molecule Representation for Predicting Drug-Target Interaction. in *Machine Learning for Healthcare Conference* vol. 106 230–248 (2019).
 30. Chen, B., Barzilay, R. & Jaakkola, T. Path-augmented graph transformer network. Preprint at <https://arxiv.org/abs/1905.12712> (2019).
 31. Vaswani, A. *et al.* Attention Is All You Need. in *Advances in Neural Information Processing Systems* (2017).
 32. Irwin, R., Dimitriadis, S., He, J. & Bjerrum, E. J. Chemformer: A pre-trained transformer for computational chemistry. *Mach Learn Sci Technol* **3**, 015022 (2022).
 33. Bjerrum, E. J. & Sattarov, B. Improving chemical autoencoder latent space and molecular de novo generation diversity with heteroencoders. *Biomolecules* **8**, 131 (2018).
 34. Honda, S., Shi, S. & Ueda, H. R. SMILES Transformer: Pre-trained Molecular Fingerprint for Low Data Drug Discovery. Preprint at <http://arxiv.org/abs/1911.04738> (2019).
 35. Nemoto, S., Mizuno, T. & Kusuhara, H. Investigation of chemical structure recognition by encoder–decoder models in learning progress. *J Cheminform* **15**, (2023).
 36. Wu, Z. *et al.* MoleculeNet: A benchmark for molecular machine learning. *Chem Sci* **9**, 513–530 (2018).
 37. Duvenaud, D. K. *et al.* Convolutional networks on graphs for learning molecular fingerprints. *Adv Neural Inf Process Syst* **28**, (2015).
 38. Williams, R. J. & Zipser, D. A Learning Algorithm for Continually Running Fully Recurrent Neural Networks. *Neural Comput* **1**, 270–280 (1989).
 39. Ucak, U. V., Ashyrmamatov, I. & Lee, J. Reconstruction of lossless molecular representations from fingerprints. *J Cheminform* **15**, (2023).
 40. Loshchilov, I. & Hutter, F. Decoupled weight decay regularization. Preprint at <https://arxiv.org/abs/1711.05101> (2017).
 41. Xiong, R. *et al.* On layer normalization in the transformer architecture. in *International Conference on Machine Learning* 10524–10533 (2020).
 42. Omote, Y., Matsushita, K., Iwakura, T., Tamura, A. & Ninomiya, T. Transformer-based approach for predicting chemical compound structures. in *Proceedings of the 1st Conference of the Asia-Pacific Chapter of the Association for Computational Linguistics and the 10th International Joint Conference on Natural Language Processing* 154–162 (2020).
 43. Wang, Y. *et al.* Identification of vital chemical information via visualization of graph neural networks. *Brief Bioinform* **24**, (2023).
 44. Jiménez-Luna, J., Skalic, M., Weskamp, N. & Schneider, G. Coloring Molecules with Explainable Artificial Intelligence for Preclinical Relevance Assessment. *J Chem Inf Model* **61**, 1083–1094 (2021).
 45. Kingma, D. P. & Ba, J. Adam: A Method for Stochastic Optimization. Preprint at <http://arxiv.org/abs/1412.6980> (2014).
 46. Ramsundar, B. *et al.* *Deep Learning for the Life Sciences*. (O’Reilly Media, 2019).
 47. Akiba, T., Sano, S., Yanase, T., Ohta, T. & Koyama, M. Optuna: A next-generation hyperparameter optimization framework. in *Proceedings of the 25th ACM SIGKDD international conference on knowledge discovery & data mining* 2623–2631 (2019).
 48. Zhou, G. *et al.* UNI-MOL: A UNIVERSAL 3D MOLECULAR REPRESENTATION LEARNING FRAMEWORK. Preprint at <https://chemrxiv.org/engage/chemrxiv/article-details/6402990d37e01856dc1d1581> (2023).
 49. Yoshikai, Y., Mizuno, T., Nemoto, S. & Kusuhara, H. Difficulty in chirality recognition for Transformer architectures learning chemical structures from string representations. mizuno-group/ChiralityMisunderstanding. <https://doi.org/10.5281/zenodo.10389855> (2023).
 50. Ramsundar, B. *MOLECULAR MACHINE LEARNING WITH DEEPCHEM*. <http://purl.stanford.edu/js264hd4826> (2018).

Acknowledgements

We thank all those who contributed to the construction of the following data sets employed in the present study such as ZINC and MoleculeNet. This work was supported by AMED under Grant Number JP 23ak0101199h0001 (TM) and JP22mk0101250h0001 (TM), and the JSPS KAKENHI Grant-in-Aid for Scientific Research (C) (grant number 21K06663, TM) from the Japan Society for the Promotion of Science.

Author Contributions

Yasuhiro Yoshikai: Methodology, Software, Investigation, Writing – Original Draft, Visualization.

Tadahaya Mizuno: Conceptualization, Resources, Supervision, Project administration, Writing – Original Draft, Writing – Review & Editing, Funding acquisition.

Shumpei Nemoto: Writing – Review & Editing.

Hiroyuki Kusuhara: Writing – Review & Editing

Competing Interests

The authors declare that they have no conflicts of interest.

Figures and Tables

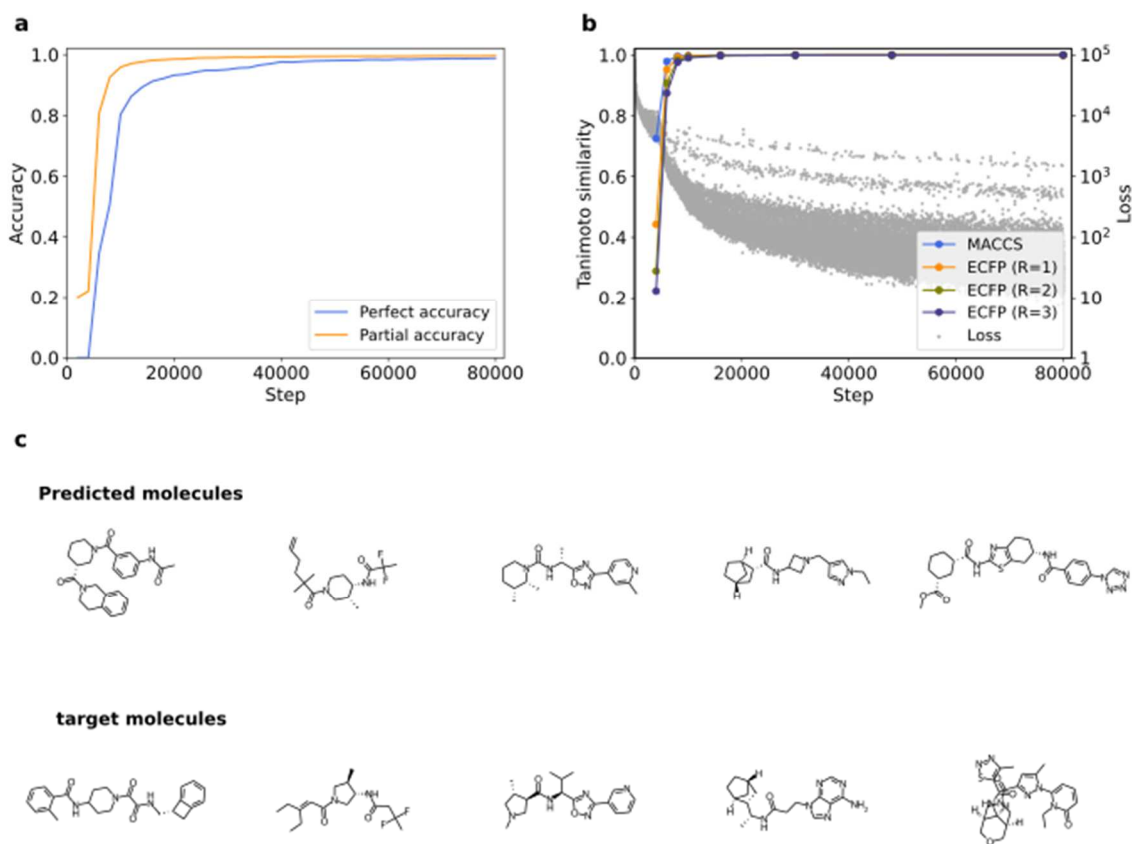


Figure 1. Partial/overall structure recognition of Transformer in learning progress

(a) Temporal change of perfect accuracy and partial accuracy. (b) Temporal change of Tanimoto similarity between the indicated fingerprints of predicted and target Simplified Molecular Input Line Entry System (SMILES), with the loss for comparison. Each gray dot indicates the loss of each batch. (c) Examples of predicted/target molecules at step 4000. Valid SMILES was filtered from SMILES in the test set predicted at step 4000, and the figure shows the randomly sampled examples of valid SMILES. Each of the molecules in the upper row is predicted targeted to the directly below molecule. Source data are provided as a Source Data file.

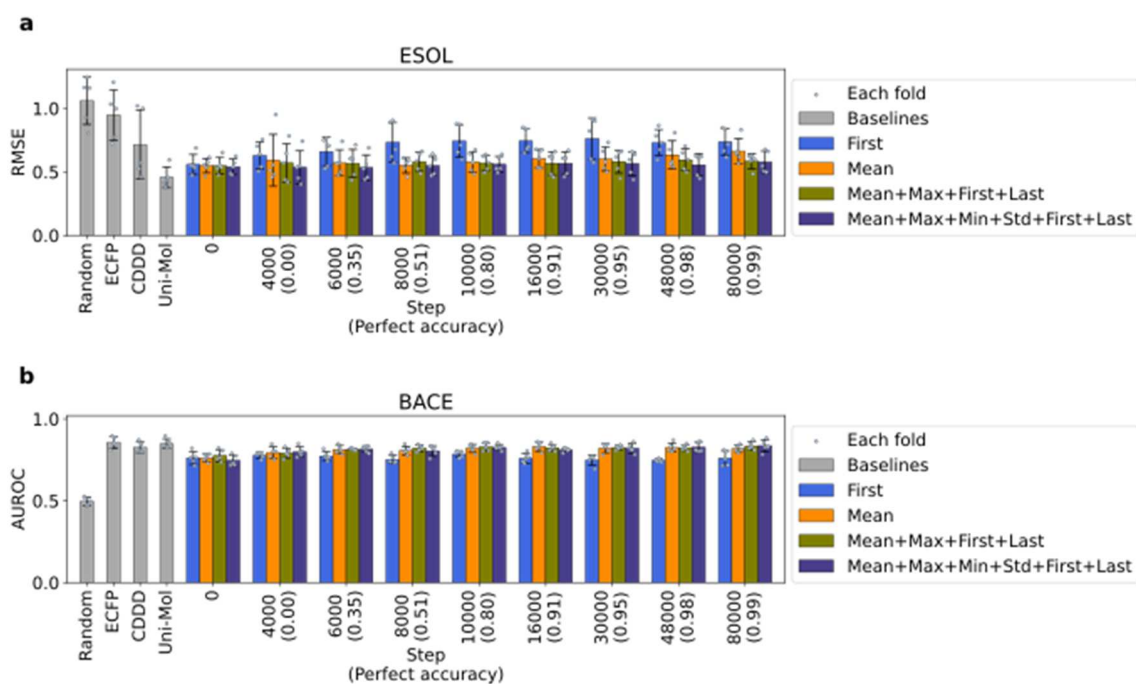


Figure 2. Performance of descriptors on molecular property prediction

(a) RMSE score of prediction on ESOL dataset from descriptors of the model at different steps of training, for 4 different ways of pooling. Blue, mean; yellow, latent representation of the first token; red, concatenation of the indicated 4 aggregation methods; navy, concatenation of the indicated 6 aggregation methods. (b) AUROC score of prediction on BACE dataset from descriptors of the model at different steps of training for 4 different ways of pooling. Mean, unbiased standard deviation and data distribution of experiments for 5 folds split by recommended method in DeepChem⁵⁰ are shown as bar height, error bar length and gray dots, respectively. The metrics were determined based on MoleculeNet³⁶. The perfect accuracy at each step is written down on the horizontal axis. Source data are provided as a Source Data file. RMSE, Root Mean Squared Error; ESOL, Estimated Solubility; AUROC, Area Under Receiver Operating Characteristic

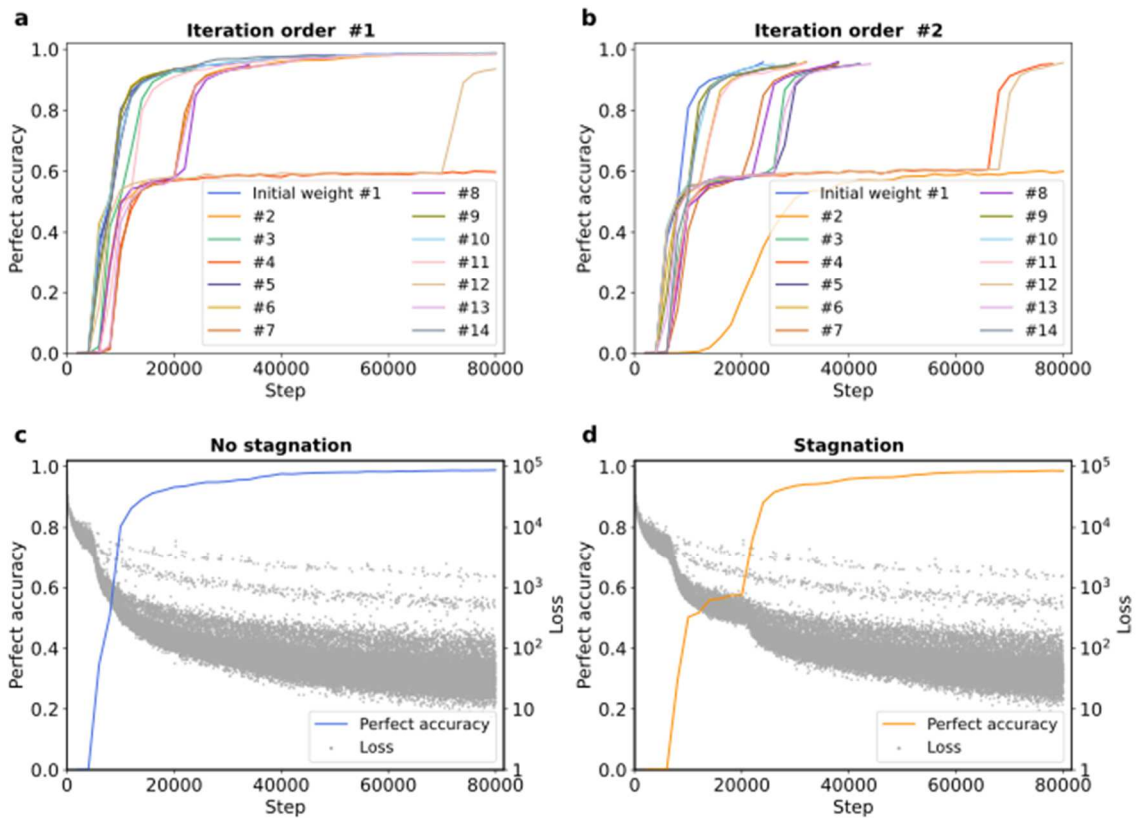


Figure 3. Stagnation of perfect accuracy at different initial weights

(a)(b) Temporal change of perfect accuracy for 14 different seeds and 2 different iteration orders. Lines with the same color corresponds to trainings from the same initial weight. (c)(d) Perfect accuracy in the trainings with/without stagnation compared to loss function. Each gray dot indicates the loss of each batch. Source data are provided as a Source Data file.

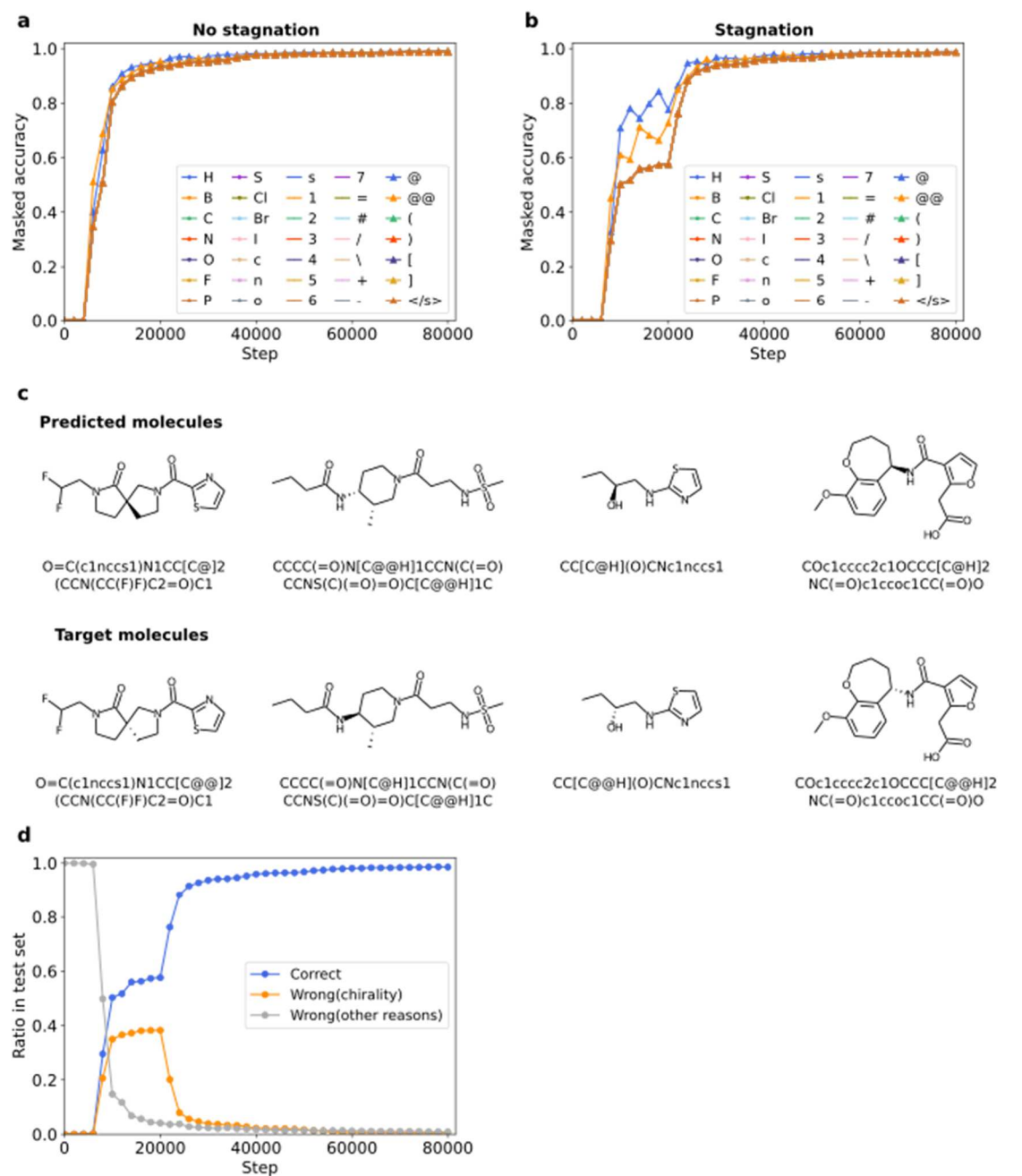


Figure 4. Difficulty in learning chirality for Transformer

(a)(b) Temporal change of perfect accuracy when each one of the characters in Simplified Molecular Input Line Entry System (SMILES) was masked for trainings in which stagnation did/did not occur. Rare tokens which did not appear in the test set are not shown. (c) Examples of target and predicted molecules during stagnation (at step 10,000). Each of the molecules in the upper row is predicted targeted to the directly below molecule. (d) Ratio of correct predictions, predictions with only mistakes of “@” token for

“@@” token and “@@” token for “@” token (mistakes attributed to chirality), and predictions with other mistakes in the test set. Source data are provided as a Source Data file.

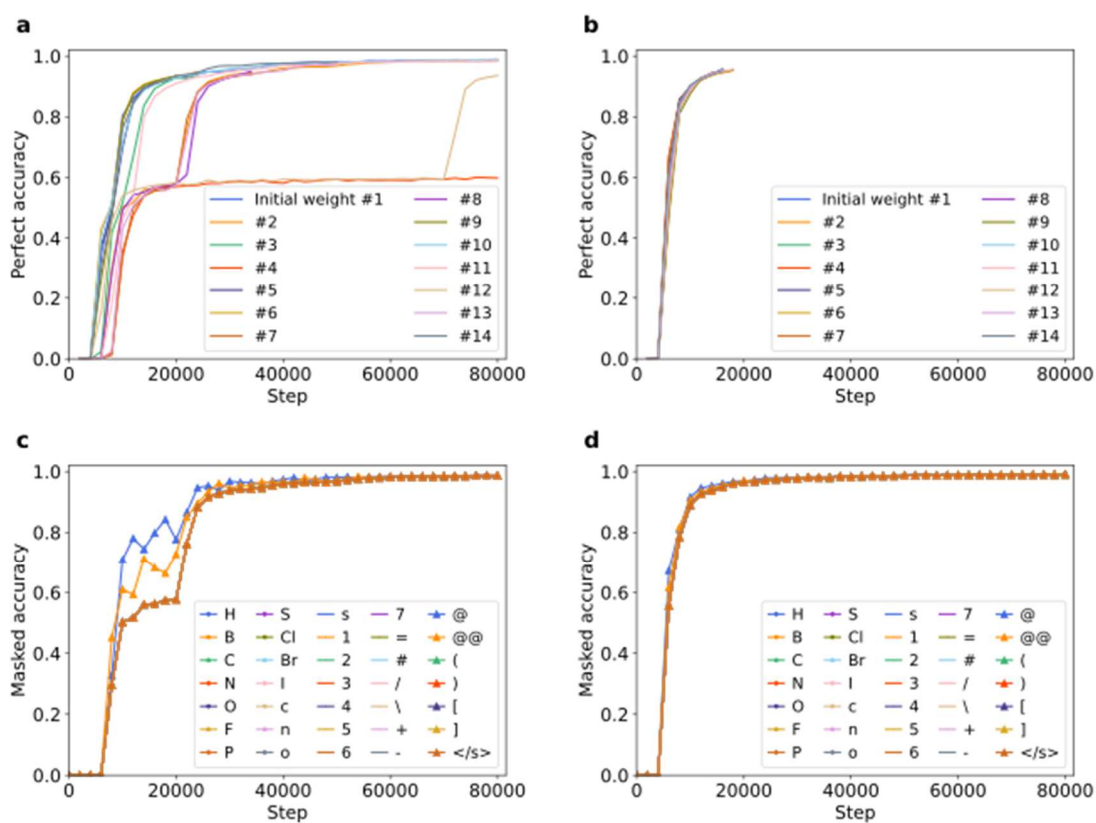


Figure 5. Improvement of stagnation and recognition of chirality by the introduction of pre-LN

(a)(b) Temporal change of perfect accuracy started from 14 different initial weights with post/pre-layer normalization(post-LN/pre-LN) structure. Lines with the same color corresponds to training from the same initial weight. (a) is reproduced from Figure 3a for comparison. (c)(d) Temporal change of perfect accuracy when each one of the characters in Simplified Molecular Input Line Entry System (SMILES) was masked for trainings with post-LN/pre-LN structure. (c) is reproduced from Figure 4b for comparison. Source data are provided as a Source Data file.

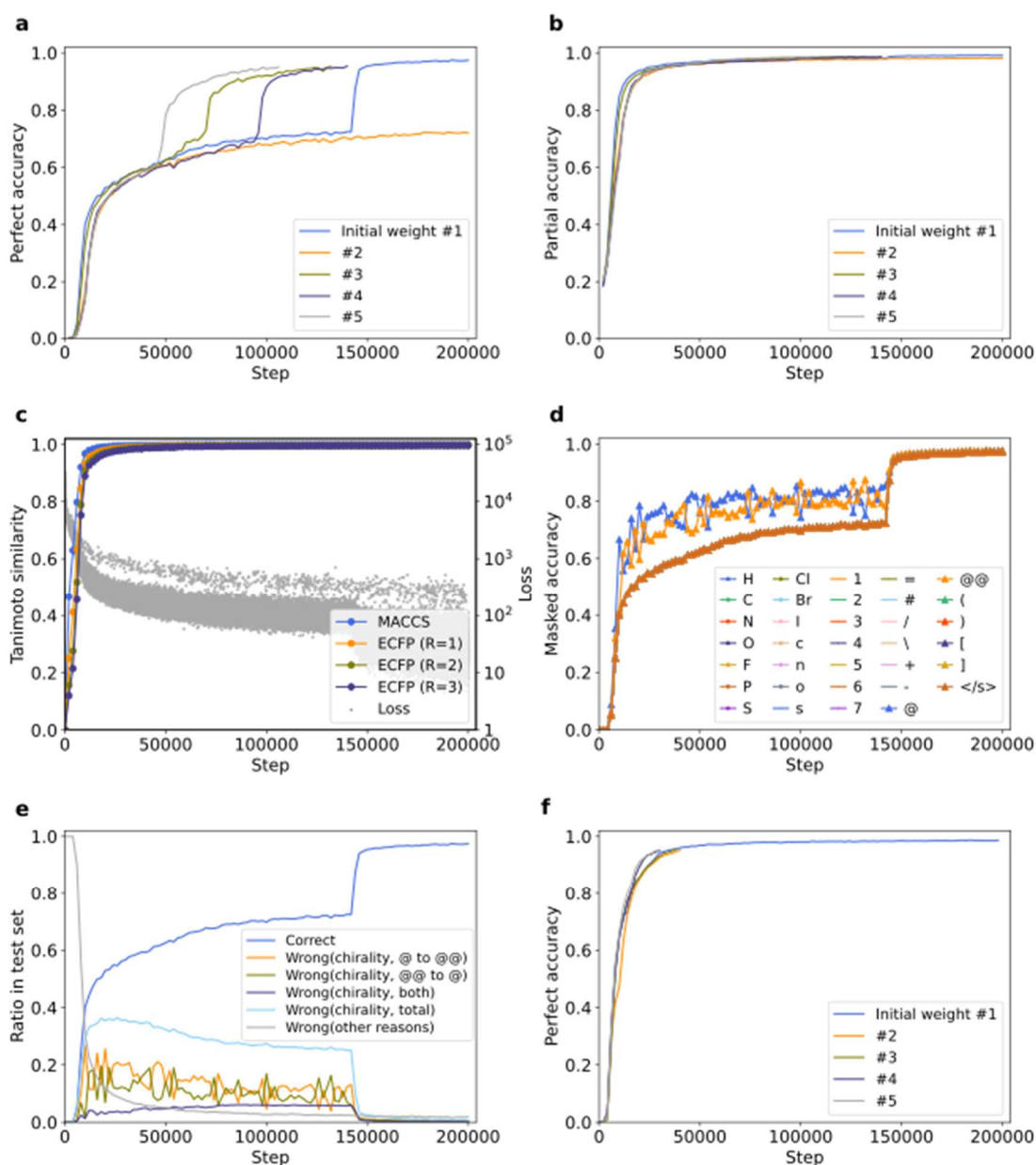


Figure 6. Experiments with the Transformer model trained by InChI-to-SMILES translation

(a) Temporal change of perfect accuracy of the model trained by InChI-to-SMILES translation started from 5 different initial weights. (b) Temporal change of partial accuracy of the model trained by InChI-to-SMILES translation started from 5 different initial weights. (c) Temporal change of Tanimoto similarity between the indicated fingerprints of predicted and target SMILES, with the loss for comparison. Each gray dot indicates the loss of each batch. (d) Temporal change of perfect accuracy when each one of the characters in SMILES was masked for one of the trainings. Rare tokens which did not appear in the test

set are not shown. (e) Ratio of molecules in the test set which were correctly predicted, and molecules which were mistakenly predicted for each reason. Wrong predictions were classified by whether they only have “@”-to-“@@” or “@@”-to-“@” mistakes, or also have other types of mistakes. (f) Temporal change of perfect accuracy and partial accuracy started from 5 different initial weights with pre-LN structure. Initial weights were not shared between post/pre-LN here. Source data are provided as a Source Data file. InChI, International Chemical Identifier; SMILES, Simplified Molecular Input Line Entry System; Pre-LN, pre-Layer Normalization

Table 1. Summary of datasets for downstream tasks

DATASET		# Total	# Used	Splitting	Task type	Recommended metric
task		molecules	molecules			
ESOL		1128	1108	Scaffold	Regression	RMSE
FreeSolv		642	628	Random	Regression	RMSE
Lipophilicity		4200	4190	Scaffold	Regression	RMSE
BACE		1513	1471	Scaffold	Classification	ROC-AUC
BBBP		2050	1899	Scaffold	Classification	ROC-AUC
ClinTox	CT_TOX	1484	1341	Random	Classification	ROC-AUC
	FDA_APPROVED	1484	1341		Classification	ROC-AUC

Table 2. Performance of each descriptor on molecular property prediction (Summary)

Descriptor	ESOL (RMSE)	FreeSolv (RMSE)	Lipophilicity (RMSE)	BACE (AUROC)	BBBP (AUROC)	ClinTox		
						CT_TOX (AUROC)	FDA_APPROVED (AUROC)	
random	1.060±0.186	1.023±0.070	1.002±0.026	0.497±0.025	0.482±0.040	0.475±0.038	0.467±0.098	
ECFP(R=2)	0.947±0.199	0.463±0.065	0.749±0.053	0.856±0.035	0.852±0.035	0.875±0.041	0.834±0.103	
CDDD	0.715±0.272	0.320±0.032	0.677±0.038	0.826±0.032	0.874±0.054	0.895±0.016	0.882±0.041	
Uni-Mol	0.456±0.082	0.295±0.032	0.505±0.053	0.847±0.029	0.861±0.042	0.874±0.048	0.875±0.053	
0	0.548±0.065	0.485±0.053	0.897±0.022	0.776±0.037	0.845±0.067	0.859±0.045	0.780±0.047	
4000	0.571±0.151	0.398±0.029	0.821±0.041	0.791±0.029	0.862±0.057	0.899±0.032	0.883±0.051	
6000	0.566±0.111	0.424±0.051	0.775±0.030	0.815±0.006	0.881±0.032	0.869±0.035	0.862±0.033	
8000	0.579±0.074	0.464±0.068	0.774±0.034	0.821±0.019	0.875±0.045	0.871±0.042	0.868±0.066	
Transformer	10000	0.570±0.063	0.459±0.065	0.782±0.034	0.829±0.025	0.859±0.064	0.837±0.062	0.819±0.065
	16000	0.567±0.091	0.486±0.064	0.804±0.033	0.823±0.020	0.876±0.047	0.876±0.023	0.804±0.088
	30000	0.581±0.091	0.497±0.104	0.793±0.024	0.825±0.012	0.863±0.082	0.845±0.032	0.799±0.049
	48000	0.594±0.086	0.496±0.047	0.801±0.033	0.824±0.019	0.875±0.043	0.888±0.025	0.850±0.049
	80000	0.585±0.059	0.461±0.058	0.771±0.024	0.835±0.024	0.861±0.062	0.904±0.024	0.894±0.046

Bold figures are the best score for each dataset among the models.

Supplementary information for “Difficulty in chirality recognition for Transformer architectures learning chemical structures from string representations”

Yasuhiro Yoshikai^{1, 3} Tadahaya Mizuno^{1, 2, 3, 4}
Shumpei Nemoto¹ Hiroyuki Kusuhara¹

¹ Laboratory of Molecular Pharmacokinetics, Graduate School of Pharmaceutical Sciences,
The University of Tokyo, 7-3-1 Hongo, Bunkyo, Tokyo, Japan

² Author to whom correspondence should be addressed.

³ These authors contributed equally.

⁴ email: tadahaya@gmail.com

Supplementary Notes

1 Related works

Chemical language models can be roughly classified into 3 categories based on their applications: structure generation (e.g., de novo drug design and retrosynthesis), end-to-end property prediction, and descriptor generation¹⁻¹⁵. The difference between the former 2 and descriptor generation from a machine learning perspective is the need for prior information. The former ones are supervised methods, whereas descriptor generation is unsupervised in general. In this regard, chemical language models for descriptor generation, which is the main topic of this study, are models that purely learn chemical structures.

Research on chemical language models with neural networks was first started in the study of Gómez-Bombarelli et al.¹⁶, which applied a variational autoencoder (VAE)¹⁷ structure to SMILES strings. They tried to represent the distribution of SMILES strings of various molecules by VAE structure, using GRU as the encoder and the decoder. Winter et al.¹⁸ generated molecular descriptors by GRU model trained for translation tasks between 2 different SMILES representations of molecules.

While the studies by Gómez-Bombarelli et al. or Winter et al. adopted the RNN model for chemical language models, the most prosperous model in the NLP study is recently becoming the Transformer¹⁹. The key feature of the Transformer model is its attention structure, in which the model processes each word attending to all words in the sentence (self-attention) or other information (cross-attention) globally. Various derivative methods have been devised based on this structure such as bidirectional encoder representations from transformers (BERT)²⁰⁻²³. Honda et al.²⁴ trained a Transformer by making it translate 2 different types of SMILES and conducted property prediction by descriptor pooled from intermediate memory in the model. Fabian et al.²⁵, based on BERT, pretrained the model not only with NLP tasks adopted in the original BERT model but also with domain-specific tasks such as fixed molecular descriptor prediction, and reported that these additional training tasks improved the performance of the model on downstream cheminformatics tasks. Irwin et al.¹⁵ pretrained a Transformer by predicting masked SMILES, translating different types of SMILES, and fine-tuned the model to predict molecular properties. The Transformer architecture is widely utilized as chemical language models for other objectives such as molecular generation¹⁻⁵ and retrosynthesis prediction⁶⁻⁹.

There are several studies to modify the Transformer structure to be suitable for recognizing chemical structures by chemical language models. One potent strategy is to combine a Transformer, or its key feature, self-attention mechanism, with 2D graph-based architecture because 2D graph representation directly provides chemical structures and high visibility of them^{10-12,14,26-28}. However, these studies focused on recognizing chemical structures in end-to-end tasks such as molecular property prediction, depending on specific tasks. To the best of our knowledge, no studies have focused on recognizing

chemical structures by chemical language models for descriptor generation, which purely learns a wide variety of chemical structures.

As will be discussed later, this paper argues that the chirality of molecules has a substantial influence on the training of the Transformer. Stereochemistry, including chirality, has been sometimes ignored in previous studies on cheminformatics¹⁸, especially when graph-based models are used, but some studies suggests that it is beneficial to incorporate information on stereoisomerism of compounds to some cheminformatics tasks. Lagnajit et al.²⁹ proposed new method for aggregating message passing neural network which takes chirality into account and showed improvement on protein-ligand docking prediction. Adams et al.³⁰ designed 3D GNN which is invariant to rotation but not to chirality, and achieved state of the art scores on chiral-related tasks.

2 Dimension-wise similarity of MACCS keys

In Partial/overall structure recognition of the Transformer in learning progress Section in the main paper, the similarities of ECFP and MACCS keys between predicted/targeted molecules were calculated, and early saturation of similarities was observed. MACCS keys are 166-bit fingerprints each of which represents whether the molecule has a certain predefined substructure. To investigate what kind of substructures are easy or difficult for the model to understand, we calculated the dimension-wise similarities between prediction and target. Here, we did not exclude molecules with invalid prediction, but instead calculated the ratio of molecules that were validly decoded and whose MACCS key bits matched between the predicted and target structures, relative to all molecules.

For each dimension i :

		Target Molecule		
		MACCS $_i$ = 0	MACCS $_i$ = 1	
Prediction	Invalid	A	D	
	Valid	MACCS $_i$ = 0	B	E
		MACCS $_i$ = 1	C	F

$$Ratio_i^0 = \frac{B}{A + B + C}$$

$$Ratio_i^1 = \frac{F}{D + E + F}$$

These scores can also remedy a limitation in the metric of the main paper which excluded molecules with invalid prediction and therefore may have filtered out complicated molecules and overestimated the similarity of fingerprints. Supplementary Figures 14 and 15 show the score for all dimensions in MACCS keys compared with their frequency (the ratio of molecules with bit 1 in each dimension). The result showed that no remarkable tendency or dimension was observed except that the ratio of correct 0/1 fingerprint is correlated to the frequency of 0/1 fingerprint in target molecules. As for temporal transition, the accuracy for most dimensions had converged to 1.0 by step 6,000, meaning almost complete reproduction of substructures. These results also support that partial structures are understood more rapidly than overall structures by the Transformer model.

3 Structure recognition and downstream task performance when stagnation occurred

In Stagnation of perfect accuracy in learning chemical structures Section in the main manuscript, we found that the perfect accuracy of the model is sometimes trapped, apparently depending on the initial weight of the model. In this section, we studied whether our findings in Sections Partial/overall structure recognition of the Transformer in learning progress and Downstream task performance in the learning progress are true for this stagnated model. We used the models in the training with initial weight #2 and iteration order #1, whose perfect accuracy transition is shown in Supplementary Figure 16a. We calculated the Tanimoto similarity of MACCS keys and ECFP and conducted molecular property prediction tasks for models when perfect accuracy reached 0.2, 0.5, 0.7, 0.9, 0.95, and 0.98 and models at steps 0, 4,000, and 80,000, just as we did in the main paper. Supplementary Figure 16b shows the Tanimoto similarity of MACCS keys and ECFP. It shows that the similarity of all fingerprints rose to nearly 1.0 at the early steps of training, while perfect accuracy and loss function is yet to converge. This result is consistent with that in Partial/overall structure recognition of the Transformer in learning progress Section. Regarding the performance of descriptors on downstream tasks, the performance did not rise in the training (Supplementary Figures 17 and 18), corresponding to the result in Downstream task performance in the learning progress Section. These results support what was suggested in the main paper, i.e., that the partial structure of the molecule is rapidly understood by the model and the performance of

the descriptor generated by the model did not change by training.

4 Training by balanced dataset about “@” and “@@” tokens

The training dataset used in the main paper was slightly biased about chiral tokens; more “@@” tokens were contained than “@” tokens. In order to clarify whether this bias is the reason for stagnation, we prepared the training dataset with balanced number of “@” and “@@” tokens and trained the model with it. We first sampled molecules from ZINC-15 in a stratified way about the length of molecules (this time “@@” was treated as a single character not to be biased). Then some of the sampled and filtered molecules were downsampled so that the distribution of “@” and “@@” tokens in canonical SMILES is symmetrical for each length. The accumulated frequency of “@” and “@@” tokens in the dataset was shown in Supplementary Figure 19a. The model was trained with this model from 5 different initial weights. The result showed that stagnation did occur in some cases (Supplementary Figure 19b), indicating that the imbalance of “@” and “@@” tokens is not the cause of difficulty and stagnation in learning chirality.

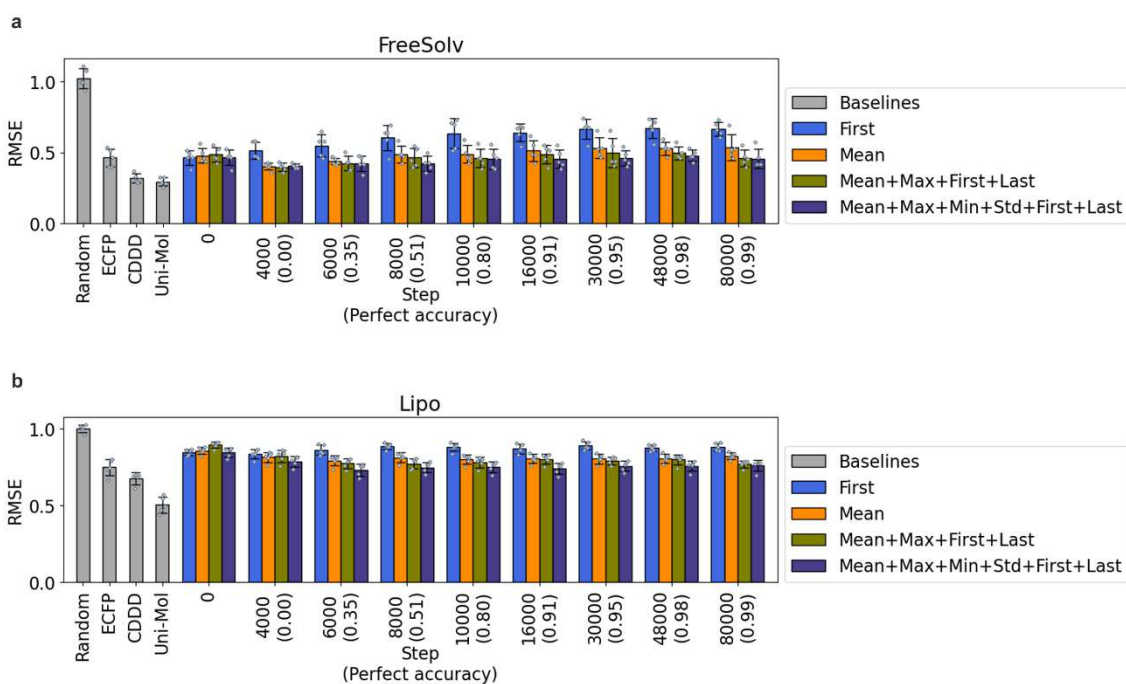
5 Training of InChI-to-SMILES translation

The molecules extracted and preprocessed from ZINC in Training a Transformer Section were used here, and we trained the Transformer model to translate InChI expression of the molecules into canonical SMILES of them. The experiments were conducted for 5 times with different initial weights. As we changed batch size according to the length of strings so that each batch contains about 25,000 tokens in this paper, relatively long InChI expression reduced batch size and extended the length of 1 epoch to 184,652.5 steps. We therefore trained the model for up to 200,000 steps, although we aborted training when perfect accuracy reached 0.95.

6 Experiments with models trained by a randomly sampled SMILES string

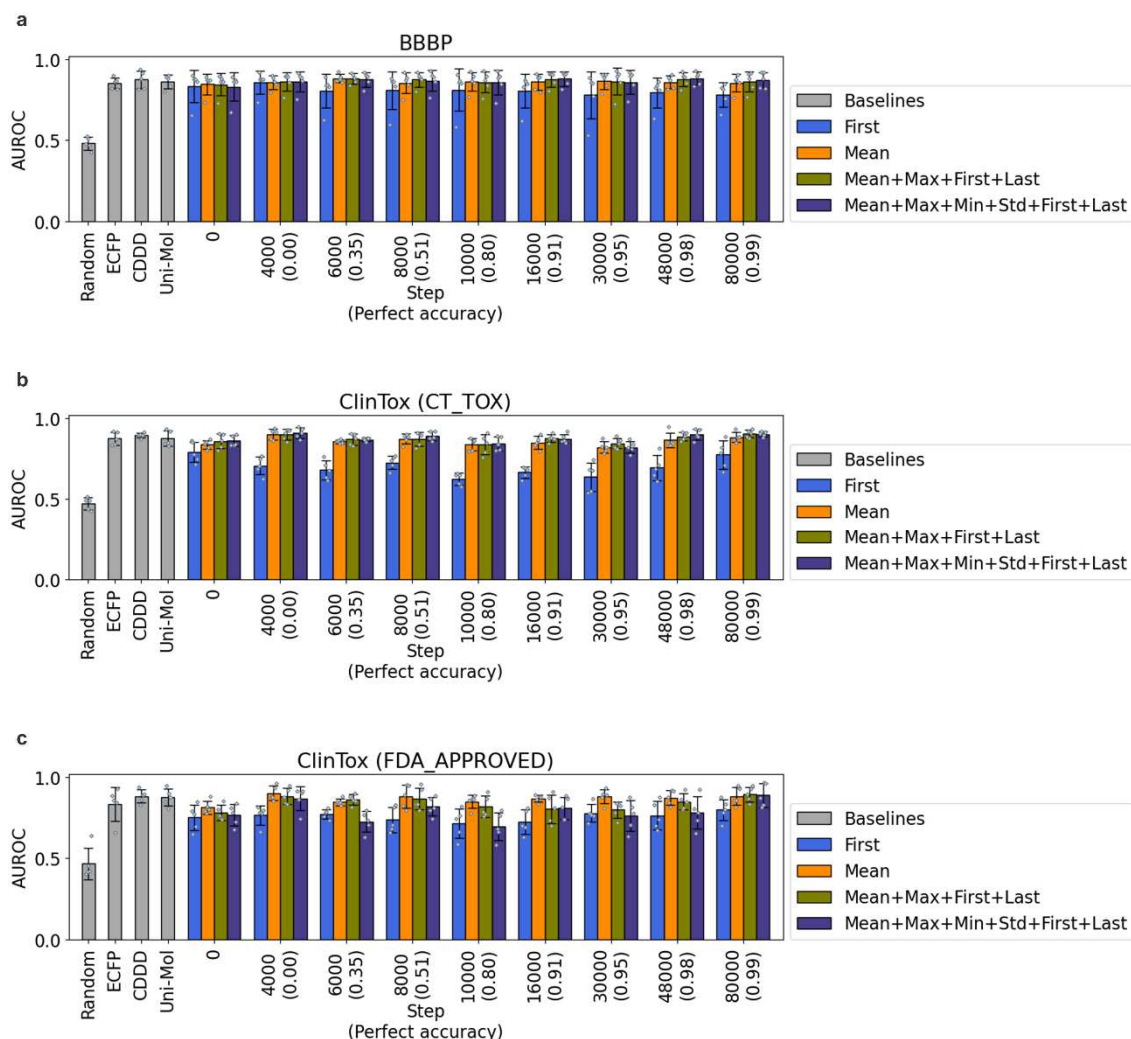
In the main manuscript, we sampled SMILES data for training and validation in a stratified way concerning the lengths of SMILES strings, which was found to enhance the translation accuracy of the trained model in our previous studies, but this sampling measure is not commonly used. To clarify whether our finding in the main manuscript depends on this sampling method, we trained the model with randomly sampled training and validation data. We filtered randomly sampled molecules as in the main paper, and 30,000,752 (about 30M) molecules were left. We sampled about 3% (8,998) molecules as test set and trained the model with the remaining molecules. 136,626 batches (68,313 steps) were contained in one epoch. We trained the model for 4 times with different initial weights and the same iteration order, and conducted some experiments in the main paper with one of the modSuplels. Supplementary Figure 20a shows the perfect accuracy for 4 trials. The result shows that stagnation did occur in some cases with this unstratified data. We then trained the model with another seed for 80,000 steps, which did not result in stagnation (Supplementary Figure 20b) and conducted some of the experiments in those sections. We compared the Tanimoto similarity of molecular fingerprints between prediction and target with steps, perfect accuracy, and loss function (Supplementary Figure 20c). The similarity almost saturated at step 10,000, where perfect accuracy and loss function had not converged. To sum up, no results remarkably different from those with stratified data were obtained, and it was suggested that the results in the main paper do not depend on how to sample the training data.

Supplementary Figures



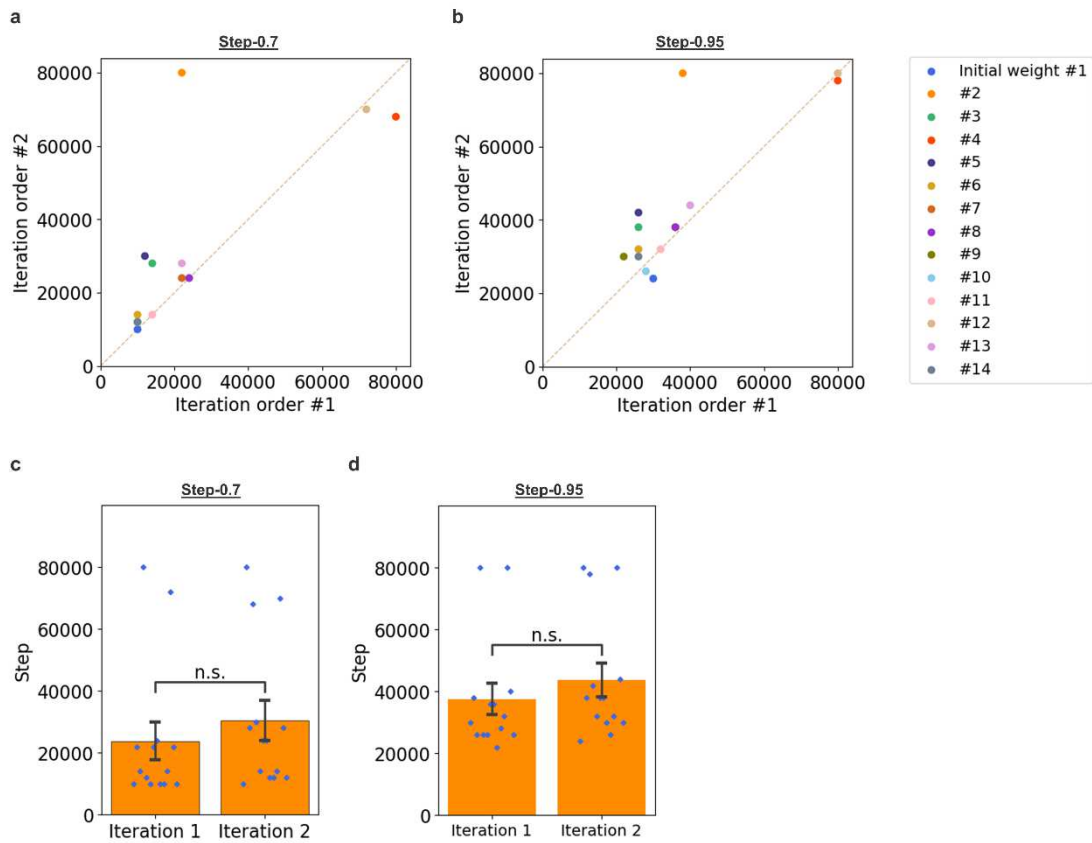
Supplementary Figure 1. Performance of descriptors on molecular property prediction (Regression task)

(a) RMSE score of prediction on FreeSolv dataset from descriptors of the model at different steps of training, for 4 different ways of pooling. Blue, mean; yellow, latent representation of the first token; red, concatenation of the indicated 4 aggregation methods; navy, concatenation of the indicated 6 aggregation methods. (b) RMSE score of prediction on Lipophilicity dataset from descriptors of the model at different steps of training for 4 different ways of pooling. Mean, unbiased standard deviation and data distribution of experiments for 5 folds split by recommended method in DeepChem³¹ are shown as bar height, error bar length and gray dots, respectively. The metrics were determined based on MoleculeNet³². The perfect accuracy at each step is written down on the horizontal axis. Source data are provided as a Source Data file. RMSE, Root Mean Squared Error; FreeSolv, Free Solvation Database



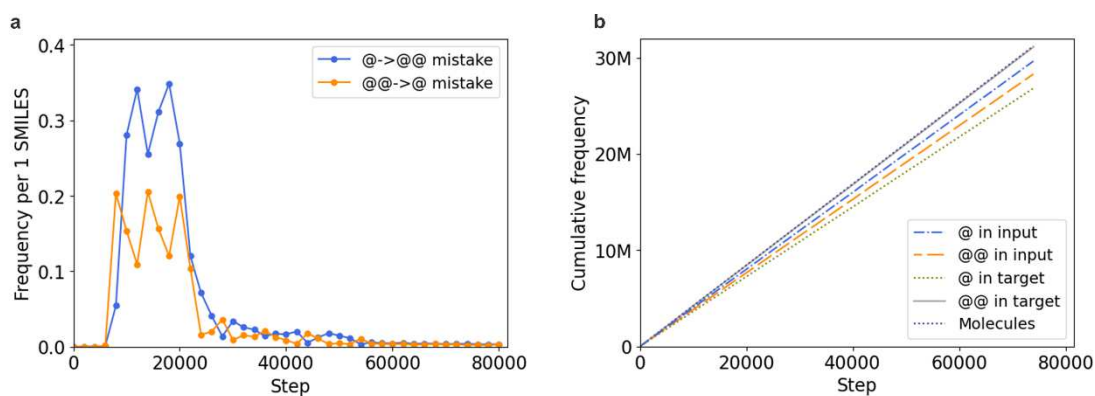
Supplementary Figure 2. Performance of descriptors on molecular property prediction (Classification task)

(a) AUROC score of prediction on BBBP dataset from descriptors of the model at different steps of training, for 4 different ways of pooling. Blue, mean; yellow, latent representation of the first token; red, concatenation of the indicated 4 aggregation methods; navy, concatenation of the indicated 6 aggregation methods. (b) AUROC score of prediction on ClinTox (failure of clinical trials for toxicity reasons) dataset from descriptors of the model at different steps of training for 4 different ways of pooling. (c) AUROC score of prediction on ClinTox (FDA approval) dataset from descriptors of the model at different steps of training for 4 different ways of pooling. Mean, unbiased standard deviation and data distribution of experiments for 5 folds split by recommended method in DeepChem³¹ are shown as bar height, error bar length and gray dots, respectively. The metrics were determined based on MoleculeNet³². The perfect accuracy at each step is written down on the horizontal axis. Source data are provided as a Source Data file. AUROC, Area Under Receiver Operating Characteristic; BBBP, The blood-brain barrier penetration; ClinTox, Clinical Toxicity; FDA, Food and Drug Administration



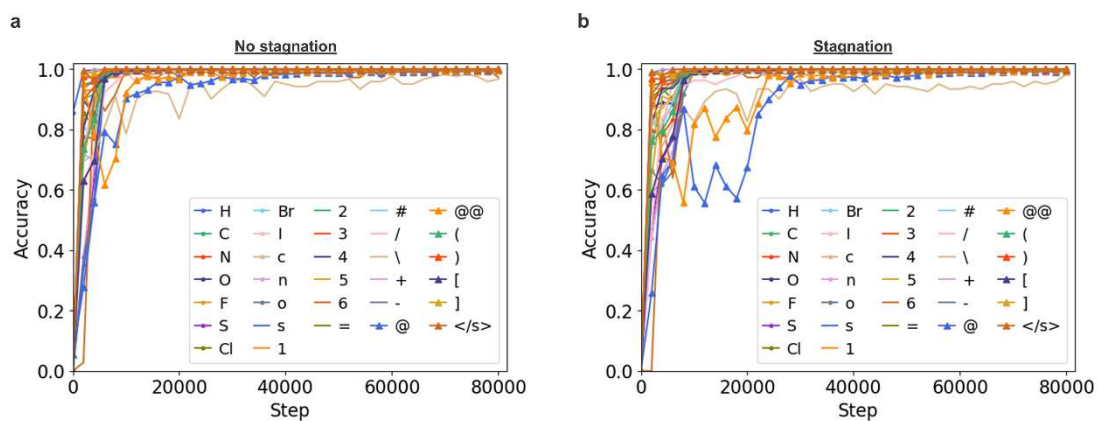
Supplementary Figure 3. Trainings with different initial weights and iteration orders

(a)(b) Comparison of *step-0.7/0.95* for each of 14 initial weights between 2 iteration orders. P values are calculated based on t-distribution with $n - 2$ degrees of freedom assuming the population correlation coefficient is 0. (c)(d) Average *step-0.7/0.95* for 14 initial weights of 2 iteration orders. Unbiased standard deviation and data distribution are shown as error bar length and blue plots, respectively. n.s. means $p > 0.05$ according to two-sided Welch's t-test. Source data are provided as a Source Data file.



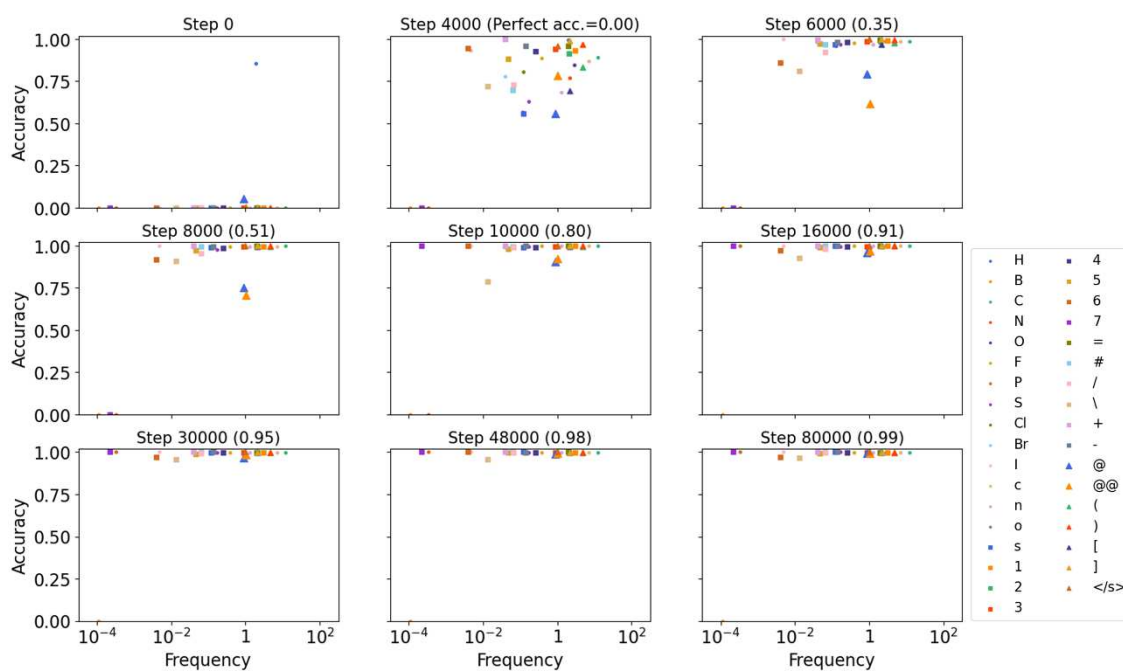
Supplementary Figure 4. Bias of “@” tokens and “@@” tokens

(a) Frequency of mistakes of “@” token for “@@” and “@@” token for “@” per one Simplified Molecular Input Line Entry System (SMILES) in the test set. Only mistakes in SMILES which was correctly predicted except chiral tokens are counted. (b) The accumulated number of molecules and “@” and “@@” tokens in each batch of the training set. Source data are provided as a Source Data file.



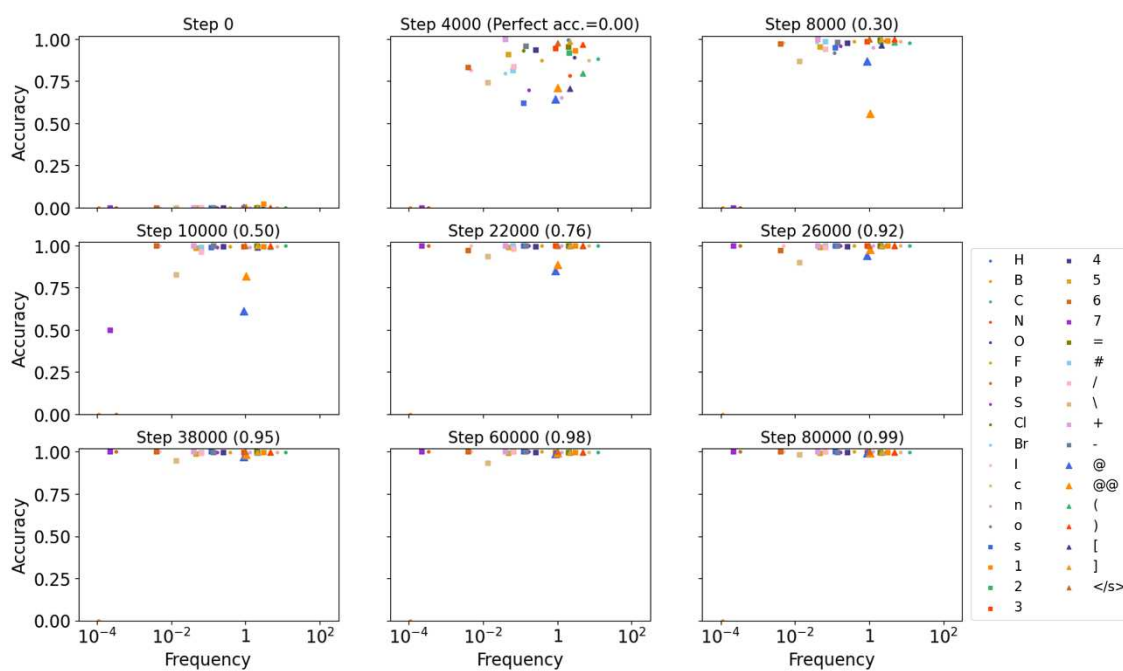
Supplementary Figure 5. Transition of character-wise accuracy with/without stagnation

(a) Transition of translation accuracy of each character when teacher-forcing was applied for a training without stagnation. (b) Transition of translation accuracy of each character when teacher-forcing was applied for a training with stagnation. Only characters with more than 10 appearances in the test set are shown. Source data are provided as a Source Data file.



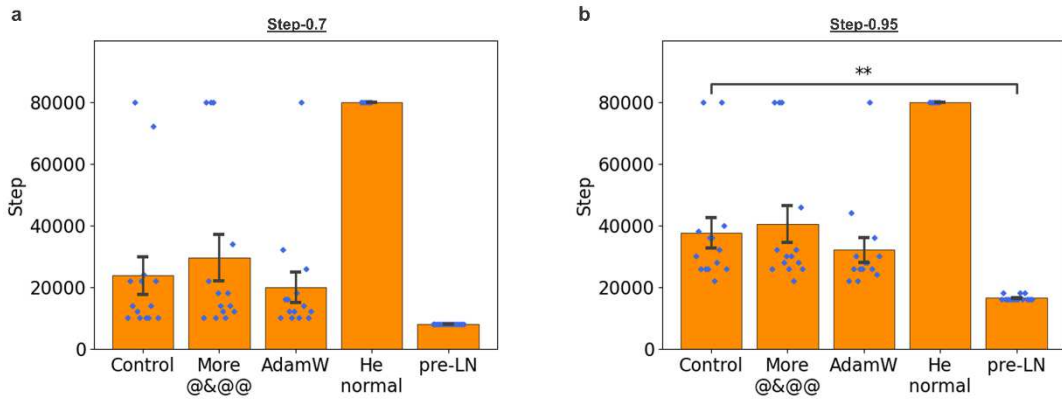
Supplementary Figure 6. Character-wise accuracy when stagnation did not occur

Translation accuracy of each character when teacher-forcing was applied for a training without stagnation. The horizontal axis shows the frequency in Simplified Molecular Input Line Entry System (SMILES) strings of the validation set, and the vertical axis shows the accuracy. Rare tokens which did not appear in the test set are not shown. Source data are provided as a Source Data file.



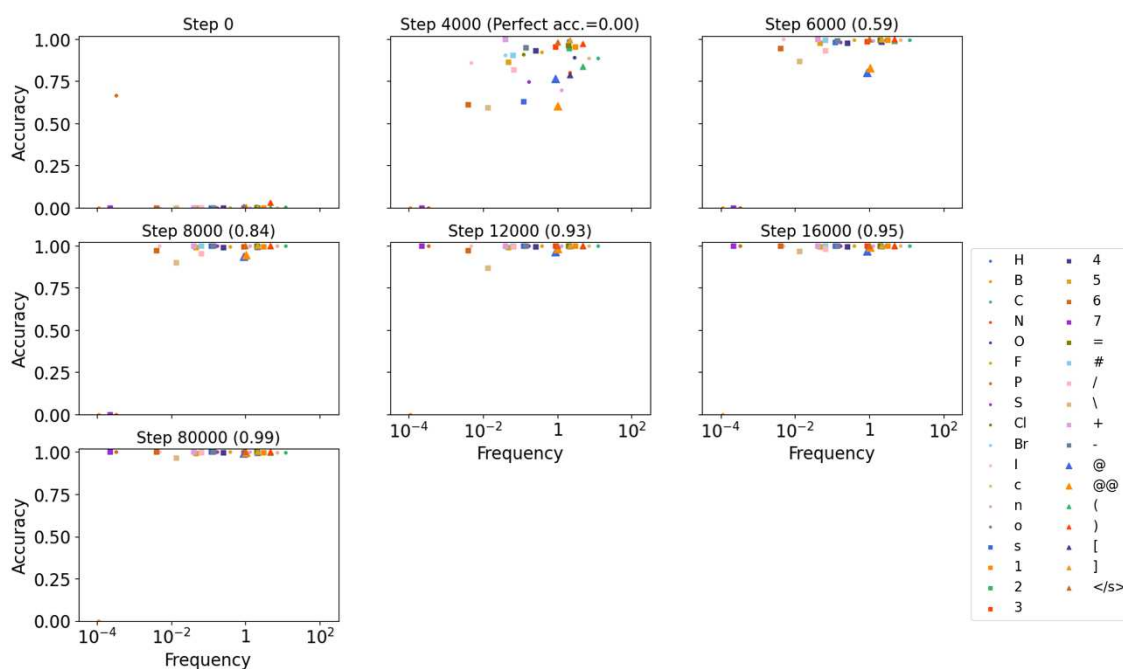
Supplementary Figure 7. Character-wise accuracy when stagnation occurred

Translation accuracy of each character when teacher-forcing was applied for a training with stagnation. The horizontal axis shows the frequency in Simplified Molecular Input Line Entry System (SMILES) strings of the validation set, and the vertical axis shows the accuracy. Rare tokens which did not appear in the test set are not shown. Source data are provided as a Source Data file.



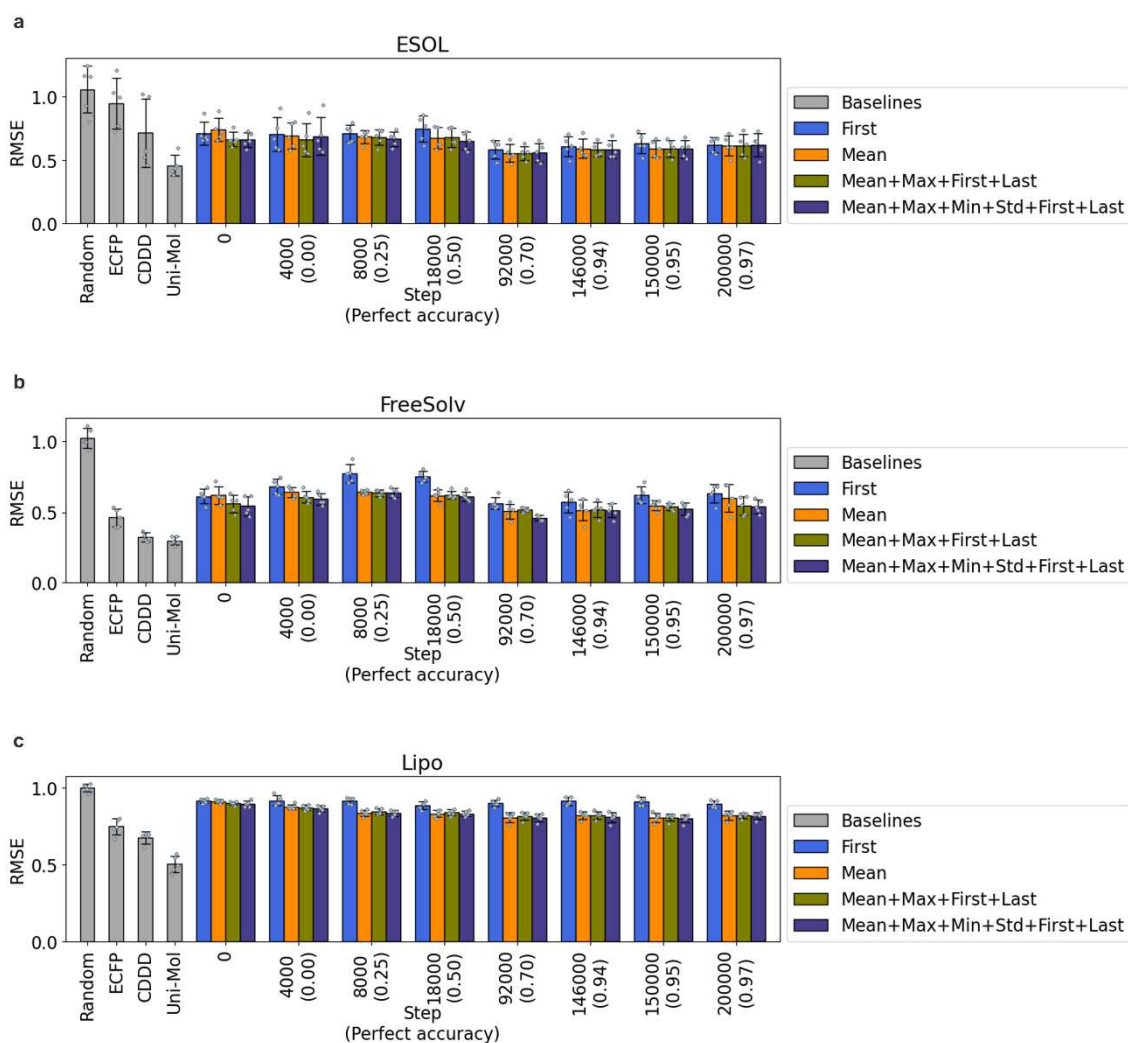
Supplementary Figure 8. Step-0.7/0.95 when 4 perturbation were applied

(a)(b) Average *step-0.7/0.95* when each of 4 perturbations was applied to 14 (or 5 for He normal) different initial weights. Unbiased standard deviation and data distribution are shown as error bar length and blue plots, respectively. ** means $p < 0.005$ according to two-sided Welch's t-test with Bonferroni correction. Source data are provided as a Source Data file.



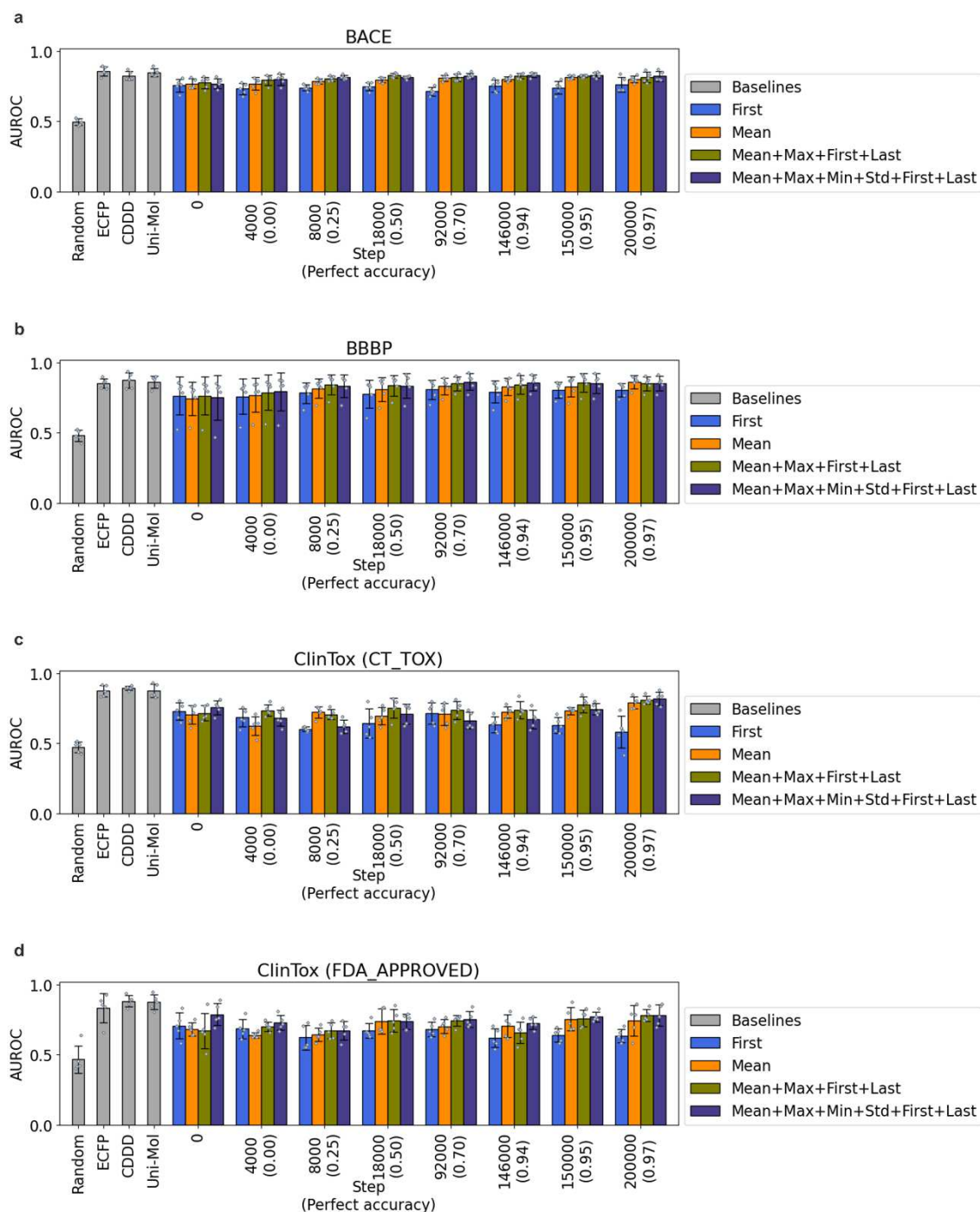
Supplementary Figure 9. Character-wise accuracy when pre-LN was introduced

Translation accuracy of each character when teacher-forcing was applied when the pre-Layer Normalization (pre-LN) structure was used. The horizontal axis shows the frequency in Simplified Molecular Input Line Entry System (SMILES) strings of the validation set, and the vertical axis shows the accuracy. Rare tokens which did not appear in the test set are not shown. Source data are provided as a Source Data file.



Supplementary Figure 10. Performance of descriptors from the model trained by InChI-to-SMILES translation on molecular property prediction (Regression task)

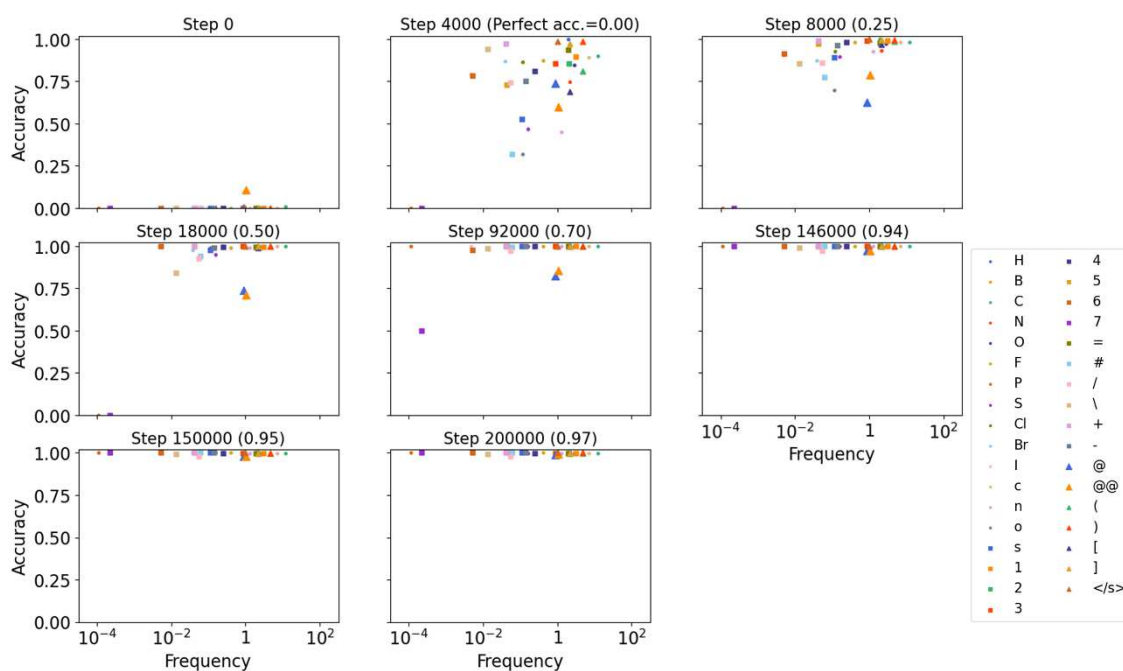
(a) RMSE score of prediction on ESOL dataset from descriptors of the model at different steps of training for 4 different ways of pooling. Blue, mean; yellow, latent representation of the first token; red, concatenation of the indicated 4 aggregation methods; navy, concatenation of the indicated 6 aggregation methods. (b) RMSE score of prediction on FreeSolv dataset from descriptors of the model at different steps of training for 4 different ways of pooling. (c) RMSE score of prediction on Lipophilicity dataset from descriptors of the model at different steps of training for 4 different ways of pooling. Mean, unbiased standard deviation and data distribution of experiments for 5 folds split by recommended method in DeepChem³¹ are shown as bar height, error bar length and gray dots, respectively. The metrics were determined based on MoleculeNet³². Perfect accuracy at each step is written down on the horizontal axis. Source data are provided as a Source Data file. InChI, International Chemical Identifier; SMILES, Simplified Molecular Input Line Entry System; RMSE, Root Mean Squared Error; ESOL, Estimated Solubility; FreeSolv, Free Solvation Database;



Supplementary Figure 11. Performance of descriptors from the model trained by InChI-to-SMILES translation on molecular property prediction (Classification task)

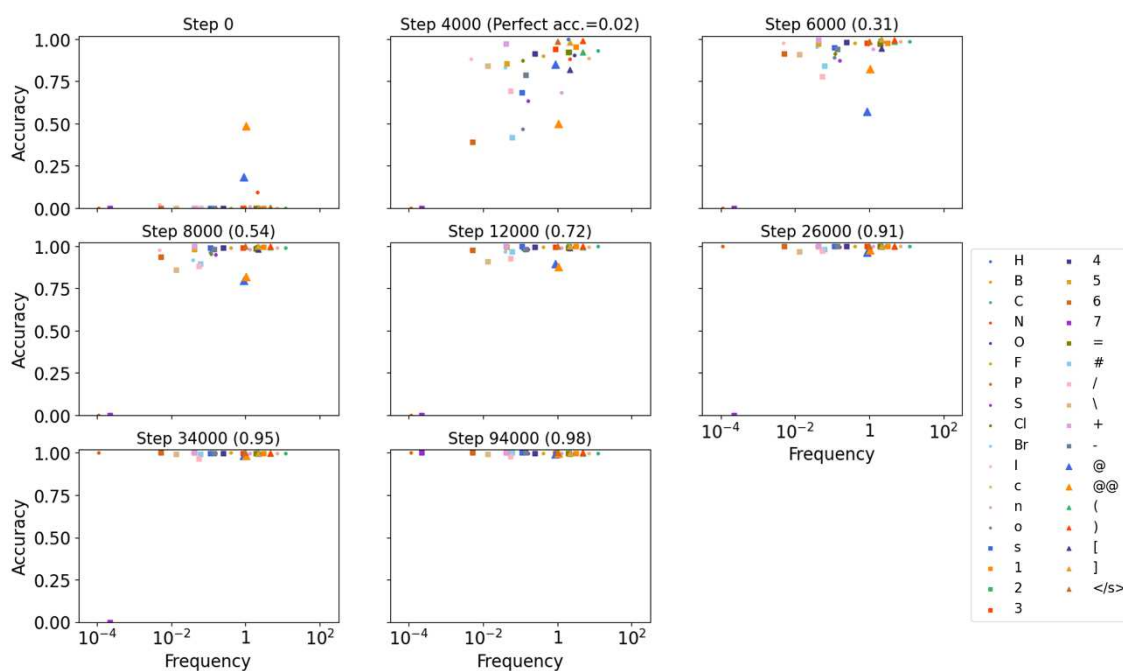
(a) AUROC score of prediction on BACE dataset from descriptors of the model at different steps of training, for 4 different ways of pooling. Blue, mean; yellow, latent representation of the first token; red, concatenation of the indicated 4 aggregation methods; navy, concatenation of the indicated 6 aggregation methods. (b) AUROC score of prediction on BBBP dataset from descriptors of the model at different steps of training, for 4 different ways of pooling. (c) AUROC score of prediction on ClinTox (failure of clinical trials for toxicity reasons) dataset from descriptors of the model at different steps of training for 4 different ways of pooling. (d) AUROC score of prediction on ClinTox (FDA approval) dataset from descriptors of the model at different steps of training for 4 different ways of pooling. Mean, unbiased standard deviation and data distribution of experiments for 5 folds split by recommended method in

DeepChem³¹ are shown as bar height, error bar length and gray dots, respectively. The metrics were determined based on MoleculeNet³². Perfect accuracy at each step is written down on the horizontal axis. Source data are provided as a Source Data file. InChI, International Chemical Identifier; SMILES, Simplified Molecular Input Line Entry System; AUROC, Area Under Receiver Operating Characteristic; BACE, Inhibitors of human beta-secretase 1; BBBP, The blood-brain barrier penetration; ClinTox, Clinical Toxicity; FDA, Food and Drug Administration



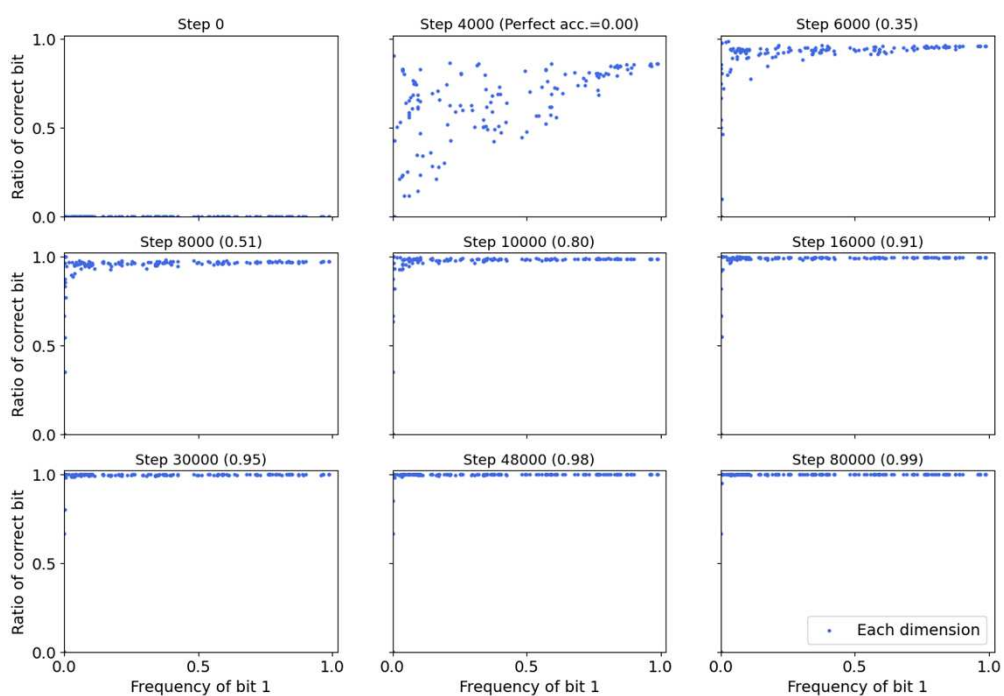
Supplementary Figure 12. Character-wise accuracy of the model trained with InChI-to-SMILES translation

Translation accuracy of each character when the model was trained to translate InChI into canonical SMILES, and teacher-forcing was applied. The horizontal axis shows the frequency in SMILES strings of the validation set, and the vertical axis shows the accuracy. Rare tokens which did not appear in the test set are not shown. Source data are provided as a Source Data file. InChI, International Chemical Identifier; SMILES, Simplified Molecular Input Line Entry System



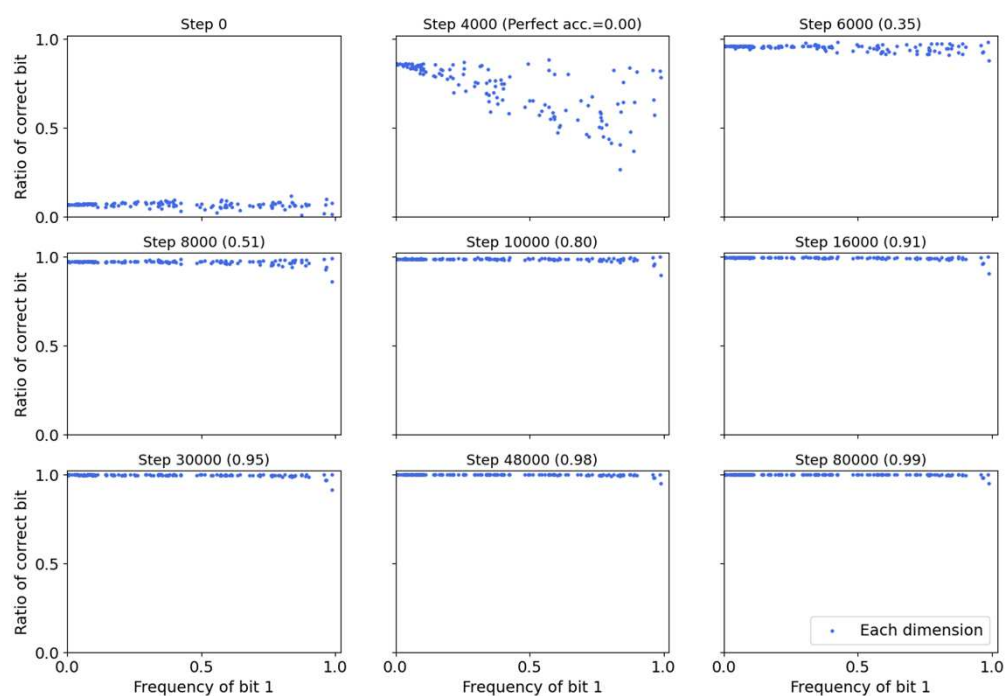
Supplementary Figure 13. Character-wise accuracy of the model with pre-LN structure trained with InChI-to-SMILES translation

Translation accuracy of each character when the model with pre-LN structure was trained to translate InChI into canonical SMILES, and teacher-forcing was applied. The horizontal axis shows the frequency in SMILES strings of the validation set, and the vertical axis shows the accuracy. Rare tokens which did not appear in the test set are not shown. Source data are provided as a Source Data file. InChI, International Chemical Identifier; SMILES, Simplified Molecular Input Line Entry System; pre-LN, Pre-Layer Normalization



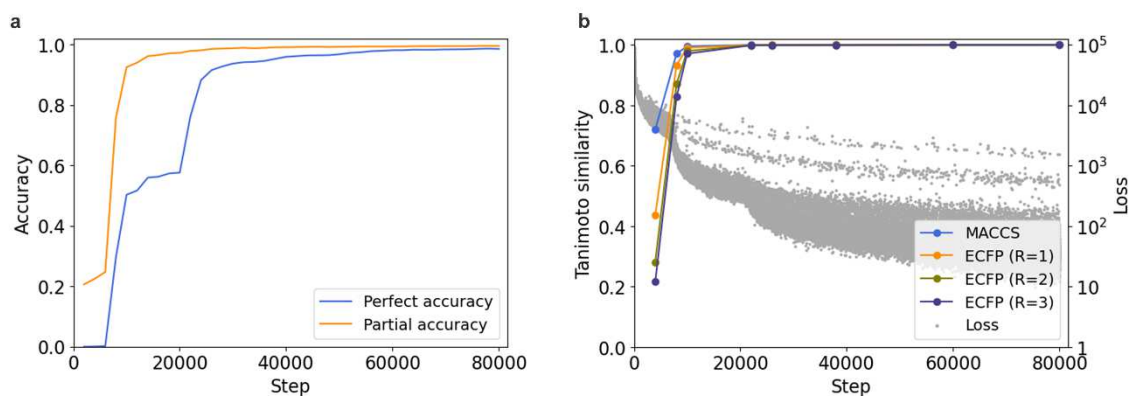
Supplementary Figure 14. Dimension-wise accuracy of MACCS keys

The ratio of molecules whose Simplified Molecular Input Line Entry System (SMILES) were validly decoded, and whose predicted/target molecules both have 1, to the number of molecules whose Molecular Access System (MACCS) keys have 1 in each dimension. The horizontal axis shows the frequency of bit 1, and the vertical axis shows the accuracy. Source data are provided as a Source Data file.



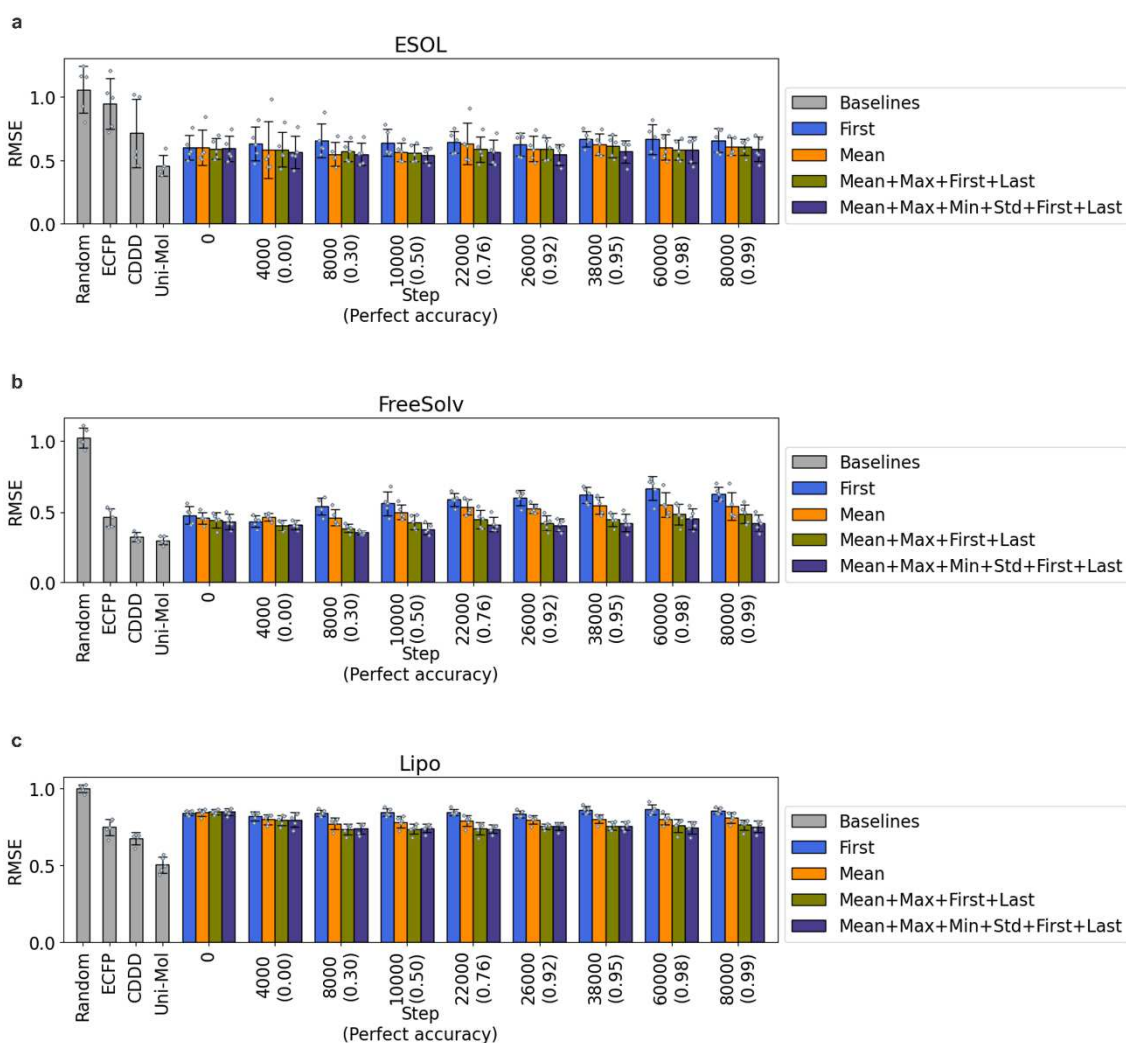
Supplementary Figure 15. Dimension-wise accuracy of MACCS keys

The ratio of molecules whose Simplified Molecular Input Line Entry System (SMILES) were validly decoded, and whose predicted/target molecules both have 0, to the number of molecules whose Molecular ACCess System (MACCS) keys have 0 in each dimension. The horizontal axis shows the frequency of bit 0, and the vertical axis shows the accuracy. Source data are provided as a Source Data file.



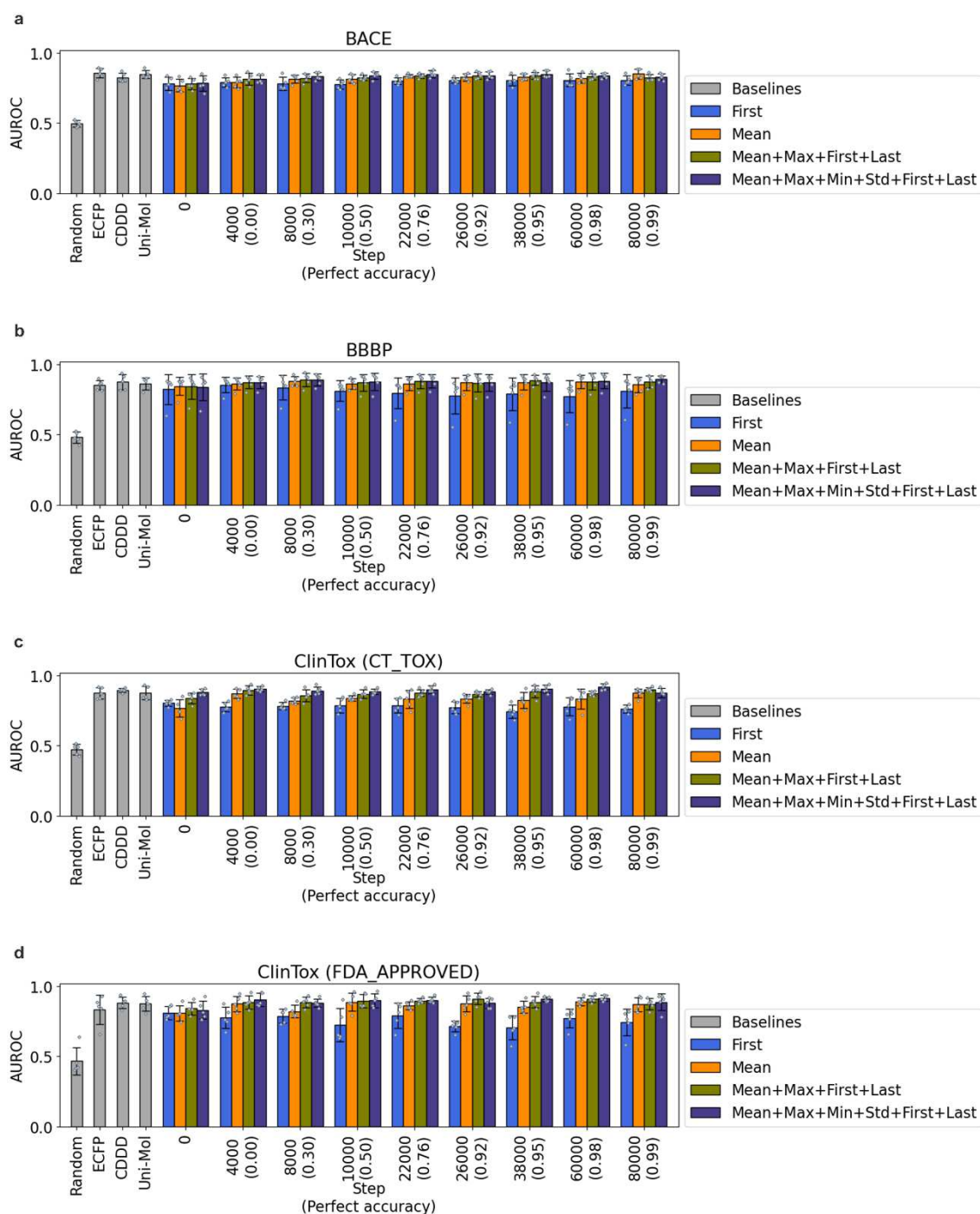
Supplementary Figure 16. Temporal change of Tanimoto similarity when stagnation occurred

(a) Temporal change of perfect/partial accuracy in the training case we used here. (b) Temporal change of Tanimoto similarity between fingerprints of predicted and target Simplified Molecular Input Line Entry System (SMILES) compared to loss function. Each gray dot indicates the loss of each batch. Source data are provided as a Source Data file.



Supplementary Figure 17. Performance of descriptors on molecular property prediction (Regression task)

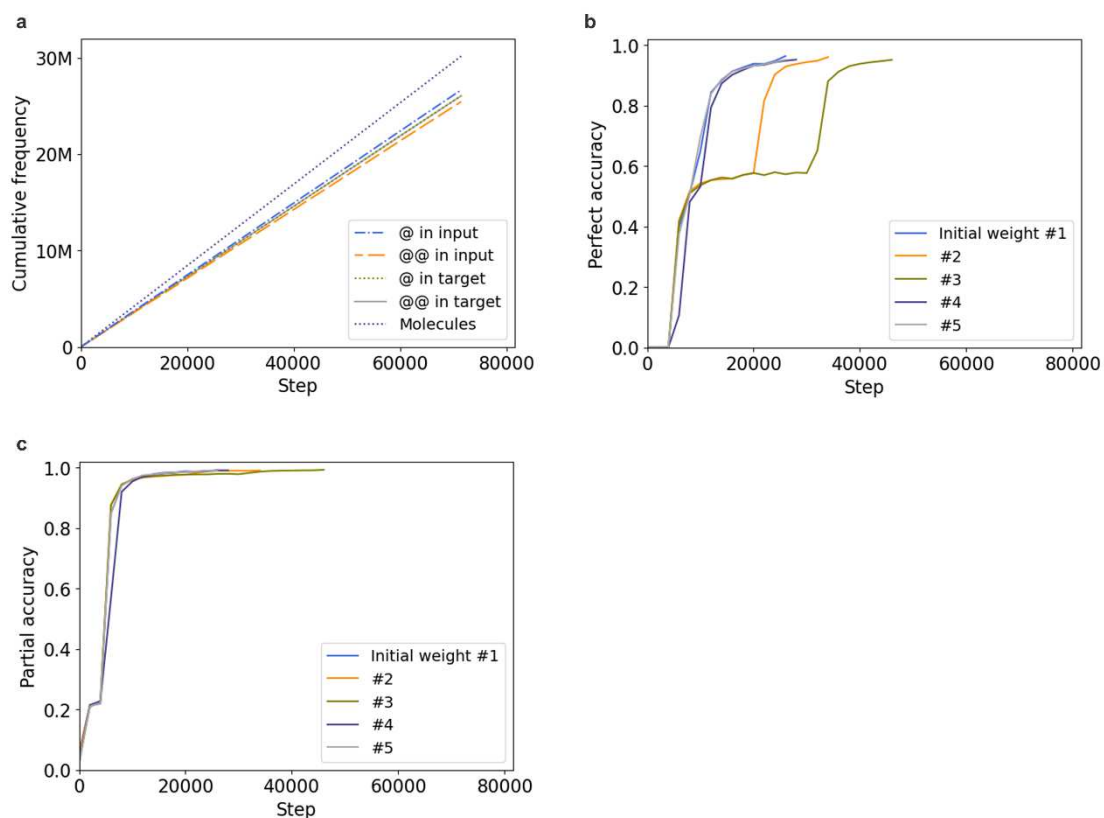
(a) RMSE score of prediction on ESOL dataset from descriptors of the model at different steps of training for 4 different ways of pooling. Blue, mean; yellow, latent representation of the first token; red, concatenation of the indicated 4 aggregation methods; navy, concatenation of the indicated 6 aggregation methods. (b) RMSE score of prediction on FreeSolv dataset from descriptors of the model at different steps of training for 4 different ways of pooling. (c) RMSE score of prediction on Lipophilicity dataset from descriptors of the model at different steps of training for 4 different ways of pooling. Mean, unbiased standard deviation and data distribution of experiments for 5 folds split by recommended method in DeepChem³¹ are shown as bar height, error bar length and gray dots, respectively. The metrics were determined based on MoleculeNet³². Perfect accuracy at each step is written down on the horizontal axis. Source data are provided as a Source Data file. RMSE, Root Mean Squared Error; ESOL, Estimated Solubility; FreeSolv, Free Solvation Database;



Supplementary Figure 18. Performance of descriptors on molecular property prediction (Classification task)

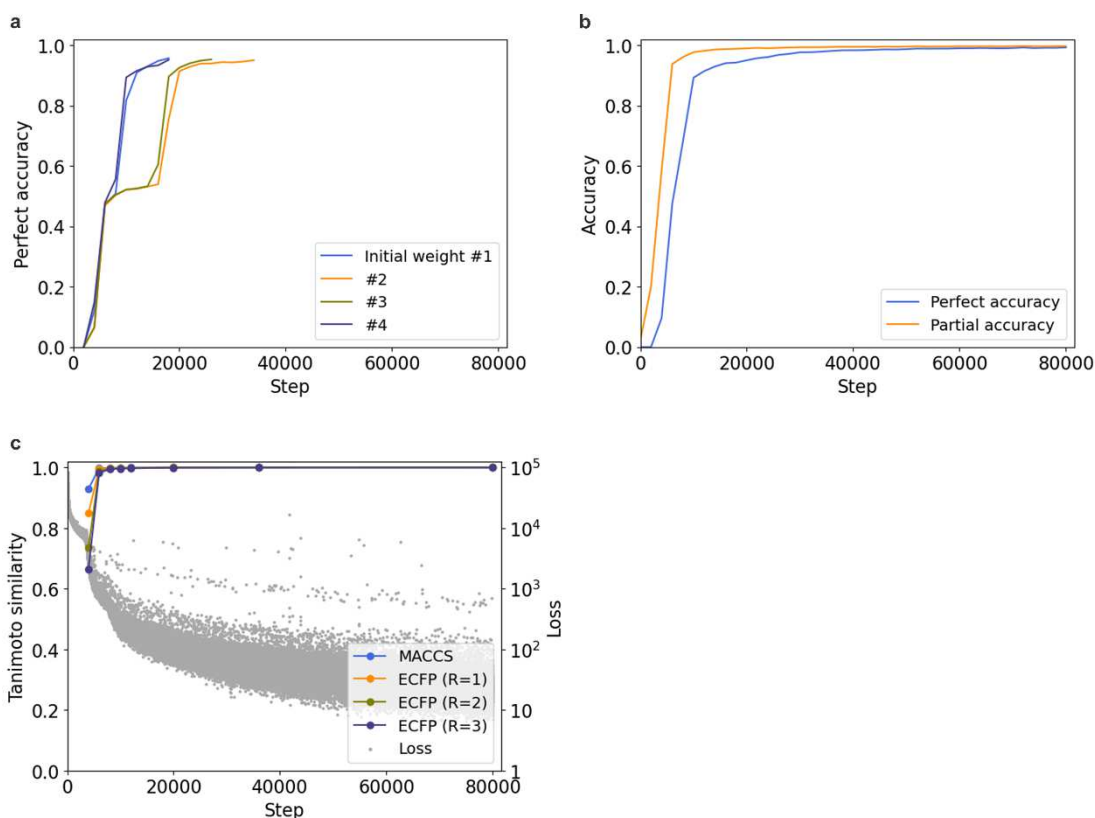
(a) AUROC score of prediction on BACE dataset from descriptors of the model at different steps of training, for 4 different ways of pooling. Blue, mean; yellow, latent representation of the first token; red, concatenation of the indicated 4 aggregation methods; navy, concatenation of the indicated 6 aggregation methods. (b) AUROC score of prediction on BBBP dataset from descriptors of the model at different steps of training, for 4 different ways of pooling. (c) AUROC score of prediction on ClinTox (failure of clinical trials for toxicity reasons) dataset from descriptors of the model at different steps of training for 4 different ways of pooling. (d) AUROC score of prediction on ClinTox (FDA approval) dataset from descriptors of the model at different steps of training for 4 different ways of pooling. Mean, unbiased standard deviation and data distribution of experiments for 5 folds split by recommended method in

DeepChem³¹ are shown as bar height, error bar length and gray dots, respectively. The metrics were determined based on MoleculeNet³². Perfect accuracy at each step is written down on the horizontal axis. Source data are provided as a Source Data file. AUROC, Area Under Receiver Operating Characteristic; BACE, Inhibitors of human beta-secretase 1; BBBP, The blood-brain barrier penetration; ClinTox, Clinical Toxicity; FDA, Food and Drug Administration



Supplementary Figure 19. Experiment with dataset containing equal number of chiral tokens

(a) The accumulated number of molecules and “@” and “@@” tokens in each batch of the training set which was downsampled so that the numbers of “@” and “@@” tokens are equal. (b) Temporal change of perfect accuracy of the model trained by the unbiased dataset started from 5 different initial weights. (c) Temporal change of perfect accuracy of the model trained by the unbiased dataset started from 5 different initial weights. Source data are provided as a Source Data file.



Supplementary Figure 20. Investigation of the effects of sampling strategy on the main results in this study

(a) Temporal change of perfect accuracy started from 4 different initial weights trained with randomly sampled molecules. (b) Perfect/partial accuracy of the training that was used for experiments. The model was trained with randomly sampled data. (c) Temporal change of Tanimoto similarity between fingerprints of predicted and target Simplified Molecular Input Line Entry System (SMILES) compared to loss function. Each gray dot indicates the loss of each batch. Source data are provided as a Source Data file.

Supplementary Tables

Supplementary Table 1. Vocabulary used to tokenize SMILES

Special tokens	<s> </s> <pad>
Normal tokens	H B C N O F P S Cl Br I c n o s 1 2 3 4 5 6 7 = / \ + - @ @ @ () []

Supplementary Table 2. Vocabulary used to tokenize InChI

Special tokens	<s> </s> <pad>
Normal tokens	H B C N O F P S Cl Br I c i o n p s b l h t q m 1 2 3 4 5 6 7 8 9 = / \ + - . , : ? # % @ @ @ () []

Supplementary References

1. Bagal, V., Aggarwal, R., Vinod, P. K. & Priyakumar, U. D. MolGPT: molecular generation using a transformer-decoder model. *J Chem Inf Model* **62**, 2064–2076 (2021).
2. Hong, Y.-B., Lee, K.-J., Heo, D. & Choi, H. Molecule Generation for Drug Discovery with New Transformer Architecture. Preprint at <https://ssrn.com/abstract=4195528> (2022).
3. Rahimovich, D. R., Qaxramon O'g'li, A. S., O'g, S. R. A. & others. Application of transformer model architecture in the new drugs design. in *2021 International Conference on Information Science and Communications Technologies (ICISCT)* 1–3 (2021).
4. Shin, B., Park, S., Bak, J. & Ho, J. C. Controlled molecule generator for optimizing multiple chemical properties. in *Proceedings of the Conference on Health, Inference, and Learning* 146–153 (2021).
5. Kim, H., Na, J. & Lee, W. B. Generative chemical transformer: neural machine learning of molecular geometric structures from chemical language via attention. *J Chem Inf Model* **61**, 5804–5814 (2021).
6. Yang, Q. *et al.* Molecular transformer unifies reaction prediction and retrosynthesis across pharma chemical space. *Chemical communications* **55**, 12152–12155 (2019).
7. Karpov, P., Godin, G. & Tetko, I. V. A transformer model for retrosynthesis. in *International Conference on Artificial Neural Networks* 817–830 (2019).
8. Zheng, S., Rao, J., Zhang, Z., Xu, J. & Yang, Y. Predicting retrosynthetic reactions using self-corrected transformer neural networks. *J Chem Inf Model* **60**, 47–55 (2019).
9. Tetko, I. v, Karpov, P., van Deursen, R. & Godin, G. State-of-the-art augmented NLP transformer models for direct and single-step retrosynthesis. *Nat Commun* **11**, 5575 (2020).
10. Mao, K. *et al.* Molecular graph enhanced transformer for retrosynthesis prediction. *Neurocomputing* **457**, 193–202 (2021).
11. Maziarka, Ł. *et al.* Molecule attention transformer. Preprint at <https://arxiv.org/abs/2002.08264> (2020).
12. Zhu, J. *et al.* Dual-view Molecule Pre-training. Preprint at <http://arxiv.org/abs/2106.10234> (2021).
13. Shin, B., Park, S., Kang, K. & Ho, J. C. Self-Attention Based Molecule Representation for Predicting Drug-Target Interaction. in *Machine Learning for Healthcare Conference* vol. 106 230–248 (2019).
14. Chen, B., Barzilay, R. & Jaakkola, T. Path-augmented graph transformer network. Preprint at <https://arxiv.org/abs/1905.12712> (2019).
15. Irwin, R., Dimitriadis, S., He, J. & Bjerrum, E. J. Chemformer: A pre-trained transformer for computational chemistry. *Mach Learn Sci Technol* **3**, 015022 (2022).
16. Gómez-Bombarelli, R. *et al.* Automatic chemical design using a data-driven continuous representation of molecules. *ACS Cent Sci* **4**, 268–276 (2018).
17. Kingma, D. P. & Welling, M. Auto-encoding variational bayes. Preprint at <https://arxiv.org/abs/1312.6114> (2013).
18. Winter, R., Montanari, F., Noé, F. & Clevert, D.-A. Learning continuous and data-driven molecular descriptors by translating equivalent chemical representations. *Chem Sci* **10**, 1692–1701 (2019).
19. Vaswani, A. *et al.* Attention Is All You Need. in *Advances in Neural Information Processing Systems* (2017).
20. Devlin, J., Chang, M.-W., Lee, K., Kristina, T. & Language, A. I. BERT: Pre-training of Deep Bidirectional Transformers for Language. Preprint at <https://arxiv.org/abs/1810.04805> (2018).
21. Lewis, M. *et al.* Bart: Denoising sequence-to-sequence pre-training for natural language generation, translation, and comprehension. Preprint at <https://arxiv.org/abs/1910.13461> (2019).
22. Lan, Z. *et al.* ALBERT: A Lite BERT for Self-supervised Learning of Language Representations. Preprint at <http://arxiv.org/abs/1909.11942> (2019).
23. Liu, Y. *et al.* Roberta: A robustly optimized bert pretraining approach. Preprint at <https://arxiv.org/abs/1907.11692> (2019).

24. Honda, S., Shi, S. & Ueda, H. R. SMILES Transformer: Pre-trained Molecular Fingerprint for Low Data Drug Discovery. Preprint at <http://arxiv.org/abs/1911.04738> (2019).
25. Fabian, B. *et al.* Molecular representation learning with language models and domain-relevant auxiliary tasks. Preprint at <http://arxiv.org/abs/2011.13230> (2020).
26. Deng, D., Lei, Z., Hong, X., Zhang, R. & Zhou, F. Describe Molecules by a Heterogeneous Graph Neural Network with Transformer-like Attention for Supervised Property Predictions. *ACS Omega* **7**, 3713–3721 (2022).
27. Chen, J., Zheng, S., Song, Y., Rao, J. & Yang, Y. Learning attributed graph representations with communicative message passing transformer. Preprint at <https://arxiv.org/abs/2107.08773> (2021).
28. Yoo, S. *et al.* Graph-Aware Transformer: Is Attention All Graphs Need? Preprint at <http://arxiv.org/abs/2006.05213> (2020).
29. Pattanaik, L. *et al.* Message Passing Networks for Molecules with Tetrahedral Chirality. Preprint at <http://arxiv.org/abs/2012.00094> (2020).
30. Adams, K., Pattanaik, L. & Coley, C. W. Learning 3D Representations of Molecular Chirality with Invariance to Bond Rotations. Preprint at <http://arxiv.org/abs/2110.04383> (2021).
31. Ramsundar, B. *MOLECULAR MACHINE LEARNING WITH DEEPCHEM*. <http://purl.stanford.edu/js264hd4826> (2018).
32. Wu, Z. *et al.* MoleculeNet: A benchmark for molecular machine learning. *Chem Sci* **9**, 513–530 (2018).